NASA TECHNICAL NOTE

NASA TN D-6021

NASA TN D-6021

A SUPERSONIC INLET-ENGINE CONTROL USING ENGINE SPEED AS A PRIMARY VARIABLE FOR CONTROLLING NORMAL SHOCK POSITION

by Francis J. Paulovich, George H. Neiner, and Ralph E. Hagedorn

Lewis Research Center
Cleveland, Ohio 44135

NATIONAL AERONAUTICS AND SPACE ADMINISTRATION • WASHINGTON, D. C. • MARCH 1971

1. Report No.	2. Government Accession No.	3. Recipient's Catalog No.
NASA TN D-6021		

4. Title and Subtitle: A SUPERSONIC INLET-ENGINE CONTROL USING ENGINE SPEED AS A PRIMARY VARIABLE FOR CONTROLLING NORMAL SHOCK POSITION

5. Report Date: March 1971

6. Performing Organization Code:

7. Author(s): Francis J. Paulovich, George H. Neiner, and Ralph E. Hagedorn

8. Performing Organization Report No.: E-5492

9. Performing Organization Name and Address:
Lewis Research Center
National Aeronautics and Space Administration
Cleveland, Ohio 44135

10. Work Unit No.: 720-03

11. Contract or Grant No.:

12. Sponsoring Agency Name and Address:
National Aeronautics and Space Administration
Washington, D.C. 20546

13. Type of Report and Period Covered: Technical Note

14. Sponsoring Agency Code:

15. Supplementary Notes:

16. Abstract

A cross-coupled inlet-engine control system concept is presented for a supersonic propulsion system consisting of a mixed-compression inlet and a turbojet engine. The control system employs manipulation of both bypass door flow area and engine speed to stabilize normal shock position in the inlet. Specifically, the case of slow-acting bypass doors used as a reset control where engine speed is the primary means of shock position control is described. Experimental results are presented showing performance of the control system with a NASA-designed inlet and a turbojet engine operating at Mach 2.5 in the Lewis 10- by 10-Foot Supersonic Wind Tunnel.

17. Key Words (Suggested by Author(s))	18. Distribution Statement
Automatic control; Supersonic inlets; Turbojet engine; Normal shock control; Propulsion system control; Supersonic inlet-engine control	Unclassified - unlimited

19. Security Classif. (of this report)	20. Security Classif. (of this page)	21. No. of Pages	22. Price*
Unclassified	Unclassified	43	$3.00

*For sale by the National Technical Information Service, Springfield, Virginia 22151

CONTENTS

	Page
SUMMARY	1
INTRODUCTION	1
APPARATUS AND PROCEDURE	3
General Description	3
Description of Engine	3
Description of Inlet	3
Description of Engine Controllers	4
Instrumentation	5
Shock Position Determination	6
Method of Testing	6
CONTROL DEVELOPMENT	7
EXPLANATION OF CONTROL ACTION	8
Control Action For a Change in Disturbance Airflow	9
Control Action For a Change in Shock Position Command	10
EXPERIMENTAL RESULTS AND DISCUSSION	10
Transient Responses	10
Decrease in disturbance airflow	11
Increase in disturbance airflow	11
Command change in shock position - move shock downstream	12
Command change in shock position - move shock upstream	12
Command change in shock position, reduced gain	12
Increase in fuel flow	13
Decrease in fuel flow	13
Sinusoidal Responses - Open Loop	13
Response of speed to a change in fuel flow	14
Response of throat exit pressure to a change in diffuser exit airflow	14
Response of throat exit pressure to a change in fuel flow	14
Sinusoidal Responses - Closed Loop	14
Response of speed to a change in speed command	14
Response of speed to a fuel flow disturbance	15
Response of throat exit pressure to a change in diffuser exit airflow	16
CONCLUDING REMARKS	17

APPENDIXES
A - Derivation of the Shape of the Closed Loop Frequency Response for Low Frequencies. 18
B - SYMBOLS 20

REFERENCES 21

A SUPERSONIC INLET-ENGINE CONTROL USING ENGINE SPEED AS A PRIMARY VARIABLE FOR CONTROLLING NORMAL SHOCK POSITION

by Francis J. Paulovich, George H. Neiner, and Ralph E. Hagedorn

Lewis Research Center

SUMMARY

A cross-coupled inlet-engine control system concept is presented for a supersonic propulsion system consisting of a mixed-compression inlet and a turbojet engine. The control system employs manipulation of both bypass door flow area and engine speed to stabilize normal shock position in the inlet. Specifically, the case of slow-acting bypass doors used as a reset control where engine speed is the primary means of shock position control is described. This control concept has the significant advantage of being able to utilize the usually fast, engine fuel-control-valving mechanism to control shock position through engine speed. It thus permits the use of a slow-bypass-door control system with its attendant reductions in cost, weight, and complexity.

Experimental results are presented which show the performance of the control system with a NASA-designed mixed-compression inlet coupled to a commercially available single rotor turbojet engine in the 4000-pound (18 000-N) thrust class, operating at a Mach number of 2.5 in the Lewis 10- by 10-Foot Supersonic Wind Tunnel. Performance of the control for disturbances in diffuser exit airflow, engine fuel flow, and changes in shock position command are presented. Both step functions and sinusoidal disturbances were used. The control is shown to operate satisfactorily, returning the inlet quickly to design conditions.

INTRODUCTION

In a supersonic airbreathing propulsion system incorporating a mixed-compression inlet and a turbojet or turbofan engine, it is essential that the inlet be operated with its normal shock located close to the aerodynamic throat in order that high operating efficiency may be obtained. Slight disturbances can cause the shock to move ahead of the throat and unstart the inlet. This event can be avoided in most cases by manipulating

the overboard bypass doors at the diffuser exit to stabilize the position of the shock. To tolerate very large-amplitude and/or very fast disturbances, a high-performance servo-system is required for manipulation of the doors. These systems are usually complex and heavy. Such high-performance bypass-door control systems have been investigated in references 1 and 2.

Conventional supersonic propulsion system controls separate the inlet controls from the engine controls. However, since the match of airflow between the inlet and the engine is affected by both engine speed and bypass door position, it would appear that a cross-coupled inlet and engine control could have merit. Cross-coupling of inlet and engine controls for future aircraft has been suggested in reference 3.

Recognizing this, and because the engine and inlet have other interrelated operating characteristics, an experimental program has been initiated to investigate various cross-coupled schemes. One promising cross-coupled scheme uses fast-acting bypass doors in conjunction with a slow reset of engine speed. Engine speed is used as a large-amplitude slow reset, to continuously return the fast doors to their most advantageous operating position. This control technique was investigated experimentally and is documented in a companion report to this one (ref. 4).

A second cross-coupled scheme uses engine speed as the fast-acting parameter with a slow reset on bypass door position. In this case, engine speed is rapidly changed to control shock position and the bypass doors are slowly reset to return engine speed to its initial commanded value. As a limiting example of this principle, the doors are set at a fixed position, leaving engine speed as the only parameter for controlling shock position. This might be representative of a discrete position bypass system, or of one which is inoperative. This scheme takes advantage of the fact that most fuel controls are inherently capable of making rapid changes in fuel flow. The change in fuel flow changes engine speed and engine airflow, and therefore has a direct effect on normal shock position. Thus, it is possible to use a slow-bypass-door control system with the attendant reductions in cost, weight, and complexity. This second type of control scheme has been investigated experimentally and is reported in this technical note.

The control scheme is intended for use when the inlet is operating in the started mode. Control functions for off-design conditions such as buzz supression, restart, and external compression operations are not discussed. No comparison is made between this scheme and conventional controls regarding factors such as performance, cost, weight, and reliability. The intent of this report is to present a concept and not a control for a specific propulsion system.

Experimental data are reported showing responses of the control for small disturbances originating downstream of the normal shock. The initial shock position was set far enough supercritically so that disturbances could be put into the system without causing inlet unstart.

APPARATUS AND PROCEDURE

General Description

Tests were conducted on a NASA-designed supersonic inlet and a General Electric model J85-13 turbojet engine, in the Lewis 10- by 10-Foot Supersonic Wind Tunnel. Nominal free-stream conditions were Mach number, 2.5; total pressure, 9.5 newtons per square centimeter; total temperature, 300 K; Reynolds number, 4.5×10^6 based on the cowl lip diameter; and specific-heat ratio, 1.4. The engine operated from 85 to 88 percent corrected speed. The data were taken with the tunnel operating on its propulsion cycle. In this cycle, the airflow downstream of the test section is vented to the atmosphere, rather than recirculated as in the aerodynamic cycle. The inlet angle of attack was zero for all the tests. Figure 1 shows the engine and inlet, with nacelle, installed in the wind tunnel.

Description of Engine

Figure 2 shows a cutaway view of the engine and inlet. The engine was an afterburning turbojet engine; however, no afterburning operation was used. The engine has a single rotor, an eight-stage compressor, an annular combustor, and a two-stage turbine. The compressor is equipped with variable inlet guide vanes and has interstage bleed at the third, fourth, and fifth stages.

Description of Inlet

Figure 3 is a cutaway view of the inlet. The inlet was a NASA-designed axisymmetric mixed-compression type designed for Mach 2.5 operation. Sixty percent of the total supersonic area contraction occurs internally. It has a capture area of 0.176 square meter and a cowl lip radius of 0.237 meter. Its design capture corrected airflow is 16.2 kilograms per second. The steady-state performance characteristics of this inlet are reported in references 5 to 8 and its dynamic characteristics are reported in reference 9. The inlet has boundary-layer bleeds and vortex generators. The configuration of the bleeds and vortex generators is known as configuration I of reference 9.

The aft portion of the subsonic diffuser is compartmented back to the engine face by three centerbody support struts. Each compartment has a bypass flow plenum which is divided into two separate equal sections by a cowl rib. Each of the six separate sections

contains an overboard bypass door assembly and an engine cooling air ejector valve.

The moveable parts of the inlet are six sliding-plate-type overboard bypass doors, a translating centerbody, and an ejector valve used to supply engine cooling airflow. The translating centerbody and engine cooling ejector valve were held fixed at their design Mach 2.5 values for all the data presented.

Figure 4 is a cutaway view of one of the six sliding-plate overboard bypass doors. An independent servochannel was used for each door. Each servochannel consisted of the bypass door assembly with hydraulic actuator and electronic position feedback, a hydraulic servovalve, and an electronic servoamplifier. A detailed description of the servoamplifier can be found in reference 10. Three doors located 120° apart circumferentially and commanded by a common control signal were used as the bypass control doors. The remaining three doors, also driven in parallel, were used as devices for causing disturbances in bypass airflow and are called the disturbance bypass doors. A typical bypass door frequency response is shown in figure 5. The frequency response shown is for a change in bypass door position sufficient to cause a change of 1 percent of the design inlet capture airflow. The figure shows that the bypass doors are a high-response system, having an amplitude ratio which is flat within zero to -3 decibels from dc to 100 hertz.

Description of Engine Controllers

The engine's fuel control was not suited for this research investigation. It is a hydromechanical control having fixed inputs of power lever angle, speed, compressor discharge pressure, and compressor inlet temperature. There was no reasonable way to introduce the signals used in this investigation into the fuel control. Consequently, an auxiliary fuel system was used. This system is shown in figure 6. Fuel flow out of the engine's main fuel control was routed from the nacelle and tunnel test section to a flow selector valve network. Fuel flow into the combustor could be selected by the experimenter to come either from the engine main fuel control or from the NASA-designed research fuel valve. Simultaneously, the other flow was diverted back to a fuel tank through appropriate hydraulic impedances. Thus, when combustor fuel flow came from the research fuel valve, the engine fuel control was functioning as though it were metering flow into the combustor, but this flow was actually being returned to the fuel tank.

The research fuel valve employs a high-performance electrohydraulic servosystem to position a fuel-metering shaft. A rectangular slot in this shaft provides a variable-area output orifice having a flow area proportional to shaft position. A constant pressure difference across this output orifice is maintained by a spring-loaded regulating valve. Thus, valve flow is proportional to shaft position and is measurable by an integral shaft position transducer. A more detailed explanation of the research fuel valve is given in

reference 11. A typical frequency response of shaft position to command voltage for ±1.5 percent of full stroke excursion is shown in figure 7.

Since the fuel valve was located approximately 7 meters away from the fuel spray nozzles and was connected by both rigid and flexible lines, line dynamics were introduced into the system. Figures 8(a) and (b) show the response of fuel spray nozzle pressure to fuel valve command voltage, showing these dynamics. The response was for a ±3 percent change in spray nozzle pressure caused by a ±1.5 percent change of the fuel valves' full stroke.

For the data in this report, the exhaust nozzle control and compressor variable geometry control operated according to their normal schedules. On this engine, the exhaust nozzle control is one section of the afterburner fuel control. The exhaust nozzle control is primarily a function of power lever position with a turbine discharge temperature override. The data presented in this report are for a fixed-power-lever position and were taken below the turbine discharge temperature override; hence, they are for a constant exhaust-nozzle area.

The compressor variable-geometry control system consists of hydraulic actuators driving a linkage mechanism which manipulates the compressor bleed doors and simultaneously moves the trailing edges of the inlet guide vanes. The normal schedule of this control system is shown in figure 9. For the data presented in this report, this control system was operating over the narrow range shown in the figure.

Instrumentation

Figure 10 shows the location of eight throat static-pressure taps, identified as taps a to h, which were used for determining shock position. Also shown in figure 10 is the location of the throat exit static-pressure tap p_{56}. This pressure tap was located 56.13 centimeters from the cowl lip and was used as an inlet control signal. The pressure signal came from a closely coupled dc strain-gage-type pressure transducer. The transducer and its associated tubing have frequency response characteristics which are flat within 0 to +2 decibels from 0 to 250 hertz, for the amplitudes presented herein.

Compressor discharge total pressure was also measured by a dc strain-gage-type pressure transducer. Its response along with its associated tubing was flat within 0 to +2 decibels from 0 to 150 hertz for the amplitudes presented herein.

Engine speed was measured by an electromagnetic pickup which was mounted adjacent to a spur gear driven by the engine gearbox. The pulse-type output from the pickup was converted to a dc signal by a frequency-to-dc converter. The speed-measuring circuit had a 1-millisecond time constant for a 5 percent step change in speed.

Shock Position Determination

Throat exit static pressure p_{56} was used as a measure of shock position for control purposes. Figure 11 shows this pressure as a function of shock position. Normally the shock was positioned 43 centimeters downstream of the cowl lip. As the shock moved upstream and downstream of this point, the control performed satisfactorily, despite the significant changes in the slope of the curve (signal gain), as is shown later.

Figure 11 was determined from the pressure profile of the eight throat static pressures (shown in fig. 10) and the static pressure p_{56}. The profile was generated by slowly ramping the bypass doors open, causing the shock to move more and more supercritical and simultaneously recording the outputs of the aforementioned transducers. The normal shock was assumed to be just aft of a pressure tap when the pressure at the tap just reached its supersonic value. The crossplot (fig. 11) was then made of the actual shock position as a function of pressure p_{56}. The circular symbols in figure 11 correspond to the pressures taken at the locations of the eight static taps. This came about because the actual shock position was known accurately for these discrete locations of the normal shock.

Another method of determining shock position was by use of an electronic shock position sensor described in reference 12. This sensor detects shock position by sensing minimums in the cowl-surface static-pressure profile using the same static-pressure signals shown in figure 10. The sensor provides useful shock position information when the shock is located from 39 to 45 centimeters from the cowl lip. The sensors output is an electronic signal, stepwise proportional to shock position.

Method of Testing

The data presented herein are the results of two types of testing, namely small step disturbances and swept frequency sinusoidal disturbances. All data were recorded on magnetic tape and processed later. All the disturbances were downstream of the normal shock as no methods were available to cause upstream disturbances. Nominal disturbance amplitudes caused approximately a 7 percent change in fuel flow or approximately a 1 percent change in the ratio of bypass flow to capture flow. The engine operating conditions were mechanical speed from 87 to 90 percent of its rated speed of 16 500 rpm with compressor inlet temperatures from 297 to 305 K resulting in corrected speeds from 85.4 to 87.5 percent. Compressor inlet total pressure varied from 7.98 to 8.16 newtons per square centimeter and compressor pressure ratio varied from 3.96 to 4.32.

Transient data were obtained by applying step-type disturbances to various portions of the control or with step disturbances in bypass corrected airflow caused by changes in

the disturbance bypass door position. Frequency response data were obtained by applying swept frequency sinusoidal disturbances to various portions of the control and to the disturbance bypass doors. The sweep rate was 1 decade per minute over the range of 1 to 140 hertz. The sweep frequency technique described in reference 13 was used in preference to testing at discrete frequencies because it resulted in a considerable reduction of tunnel running time. This method provided on-line polar frequency response plots. Also, it permitted off-line plotting of Bode-type frequency response plots from the tape recorded signals. The frequency response data below 1 hertz were obtained by the discrete frequency technique.

CONTROL DEVELOPMENT

Figure 12 shows a simplified block diagram of the cross-coupled control presented herein. This control is intended for use when the inlet is operating in the started mode. The control's function is to maintain the normal shock at its design position. It corrects for inadvertant flow disturbances originating from unsteady engine operation, fluctuating upstream conditions, or component drifts.

The entire control is made up of three loops. The speed loop is indicated by the light solid line. It consists of a controller acting on a speed error signal. The output of the controller changes engine fuel flow $\dot{w}_f$; which in turn changes engine speed and consequently engine airflow m_{eng}. (All symbols are defined in appendix B.) Engine speed is fed back negatively to close the loop. The error signal for the speed loop, which normally would only be the difference between the commanded speed N_{com} and the actual speed N, is modified by the addition of a speed command biasing signal N_{bias}.

The bias signal is produced by the shock position loop which is shown by the heavy solid line. This loop consists of a controller acting on a throat exit static-pressure error signal. The static pressure p_{56} is indicative of shock position. Whenever a shock position error exists, the shock position controller's output biases the speed command signal, thereby changing engine speed. The change in engine speed results in a change in diffuser exit airflow m_{de}. This acts through the inlet dynamics to change p_{56}. Pressure p_{56} is fed back negatively to close the loop. Thus, the engine speed loop can be considered as a block in the shock position control loop.

The third loop, shown by the dashed line, is the speed reset loop. This loop consists of a controller acting on an error signal which is the difference between the commanded speed and actual speed. The function of this loop is to allow engine speed to be slowly reset until it is equal to commanded speed. This is accomplished by slowly moving the control bypass doors.

The feedback loop shown at the top of the diagram indicates that the inlet total pressure H is fed back to affect the engine.

Before this control system was applied to the propulsion system in the wind tunnel, the propulsion system and control were dynamically simulated on an analog computer at the Lewis Research Center analog computing facility. Referring now to the block diagram in figure 13, the controller types and gains were established on the analog simulation from empirical relations and from limited information obtained during prior inlet tests. Controller constants were later adjusted in the wind tunnel. The control was developed by first closing the speed loop, shown by the light solid line; then closing the shock position loop, shown by the heavy solid line; and finally closing the speed reset loop, shown by the dashed line.

In the wind tunnel, the control system was implemented on a desktop-type analog computer using standard analog components. Since the control system and the controllers had all electronic inputs, command and disturbance signals were introduced as analog voltages at the appropriate summing junctions.

It was mentioned earlier that no data were taken with the afterburner in operation. For this afterburning turbojet, with the turbine nozzle operating near the choke point, high-frequency dynamics associated with the inlet, compressor, and main combustor are almost uncoupled from the afterburner and exhaust nozzle. The low-frequency and reset dynamics, as well as controls, could couple to the afterburner operation. In order to conduct a study of transients arising from operation with the afterburner, an extensive modification of the engine's afterburner fuel control would have been necessary. This provision was not made for this test program.

EXPLANATION OF CONTROL ACTION

As described earlier, the object of this control is to always maintain the shock position at its commanded position. It does this by first changing engine speed through fuel flow, and then by slowly manipulating both bypass door position and fuel flow to return speed to its commanded value. The block diagram of the system with the transfer functions used for the controllers is shown in figure 13. The speed loop used a proportional-plus-integral control with a time constant of 0.30 second. The shock position loop also used a proportional-plus-integral control with a time constant of 0.015 second. The speed reset loop used a slow integral control. Both the speed loop and the shock position loop are much faster than the speed reset loop. Therefore, for small changes in inlet airflow the action of the outer loops can drive the shock back to its commanded position before the bypass doors begin to move.

Referring again to figure 13, the control action schematic above the block diagram describes the controller action. In this schematic, control bypass door position is the ordinate and engine speed is the abscissa. The light diagonal lines represent combinations of engine speed and bypass door position for a constant position of the normal shock. This assumes constant disturbance airflow m_d and constant upstream conditions. Thus, if engine speed is increased while bypass door flow area is appropriately decreased, the sum $m_{by} + m_{eng} + m_d$ can be held constant. This results in a constant position of the normal shock. The heavy line is the operating line selected for this investigation but need not necessarily be the shape shown.

Control Action For a Change In Disturbance Airflow

Assume that the commanded speed N_{com} and the commanded pressure $p_{56,com}$ representing commanded shock position are satisfied and that the bypass doors are partly open such that the operating point is at position 1 in the schematic of figure 13. Assume there is a disturbance in inlet corrected airflow downstream of the shock. This could be represented by a decrease of disturbance airflow m_d. Such a disturbance could be caused by an anomaly in the primary burner or in the duct burner of a duct-burning turbofan. There would be a consequent decrease in diffuser exit airflow m_{de}. The normal shock would move upstream, resulting in an increase in p_{56}. The error between p_{56} and $p_{56,com}$ would produce a positive value of N_{bias}, which would result in an increase in w_f. Engine speed would increase as indicated by position 2 in the schematic. The shock would be returned approximately to its original position but actual speed would now exceed its commanded value. An error would therefore exist at the input to the bypass door controller. The bypass doors would open to increase m_{by}. As the outer loop maintains the shock near its commanded position, the bypass doors would simultaneously open as speed decreases. When the door motion ceased, the propulsion system would be operating at point 3 in the diagram.

The case of a sudden increase in disturbance airflow is also shown in the schematic. This is shown by the sequence 1-4-5, assuming the same initial conditions. The control action is converse to the action just described. The particular case shown would require the doors to move to the fully closed position just when the speed error was returned to zero. In case the initial disturbance was greater, as shown by the sequence 1-6-7, the speed error would not be completely eliminated. In this case, speed would remain at a reduced value but the normal shock would be at its commanded position.

For disturbances that cause forward shock motion, it is seen that two limits can be reached: maximum engine speed or bypass doors fully open. For the opposite disturbance, the limits are doors fully closed or engine flameout.

Control Action For a Change in Shock Position Command

Referring again to the schematic of figure 13, describing a change in shock position command to a more supercritical position would involve the following steps: Assume initial conditions correspond to position 8 in the schematic. A decrease in $p_{56,com}$ would result in a positive value for N_{bias}, increasing speed and engine airflow and displacing the shock downstream. This is represented by point 9. The increase in speed above its commanded value would produce an error at the input to the bypass door controller. The bypass doors would slowly open while the shock position loop held the shock at its new commanded position until equilibrium was reached at point 10 in the diagram.

It should be recognized that these descriptions of the action of the control are idealizations. In a real control, the trajectories would be rounded by the simultaneous action of the various loops.

EXPERIMENTAL RESULTS AND DISCUSSION

Transient Responses

Figures 14 to 23 show transient responses for portions of the control and for the complete control for step-type inputs. Step-type disturbances are the most critical for this control and would be the most severe experienced in a real system. Table I is provided as a summary of the transient responses presented. This table shows the various types of disturbances, engine and inlet initial conditions, shock position controller gain variation, and whether the particular response presented included use of the speed reset loop.

The step disturbance data presented used three values of shock position controller gain K_1, as noted in the figures and in table I. Other gain terms were held constant. No attempt was made to optimize the controller performance for all disturbances.

In figures 14 to 23, all the variables are shown with increasing values in the upward direction. The change in fuel flow is shown as a percent change of the fuel valve's full flow capability, which was 18.2×10^2 kilograms per hour. The change in compressor discharge pressure is shown as a percent change of the initial value of compressor discharge pressure.

In referring to the block diagram of figure 13, it should be recalled that shock position is not measured directly in the control but the pressure signal p_{56} was used instead. The step data show the response of p_{56} with its equivalent change in shock position.

Decrease in disturbance airflow. - Figure 14 shows a transient response for a decrease in diffuser exit airflow. For this response, the control contained no reset; that is, the control bypass door loop was deactivated. The initial operating conditions are listed in table I. The disturbance was caused by closing the disturbance bypass doors reducing m_{by}/m_0 by 1.4 percent. Door closure caused the shock to move upstream approximately 3.3 centimeters, increasing control pressure p_{56}. The control detected an error in p_{56}, requesting a value for N_{bias} to reduce the error to zero. This is seen by the increase in w_f. Pressure p_{56} was returned to its initial value within 0.20 second and speed was stabilized within 0.40 second with no speed overshoot. The control performed very stably.

Figure 15 shows a response for the same type of disturbance as figure 14, but with the reset loop active. In this case, the disturbance was slightly smaller (the absolute value is not known), causing the shock to move 2.7 centimeters upstream from the same initial position as figure 14. The sequence of events for the initial transient is the same as for figure 14 with the fast outer loop first returning the shock to its commanded position within 0.21 second; at this time, however, a maximum speed error existed in the reset loop. The control bypass doors slowly opened, reducing the speed error to zero after 1.5 seconds. It can be seen that, after the initial transient, the shock was maintained near its commanded position during the reset action.

The reset action of the control bypass doors of figure 15 shows a dead time of about 0.08 second after the initiation of a speed error signal. This dead time is due to the threshold voltage in the control bypass door servosystem and not to a built-in dead time in the speed reset loop.

Increase in disturbance airflow. - Figure 16 shows a response of the control without reset for a disturbance caused by opening the disturbance bypass doors, increasing m_{by}/m_0 by 1.4 percent and causing the shock to initially move 2.3 centimeters downstream. For this case, the shock was first returned to its commanded position in 0.12 second, and speed was stabilized in 0.28 second with slight overshoots in both speed and shock position.

When figure 16 is compared to figure 14, it can be seen that the change in control pressure p_{56} was 2.4 times as great for figure 16 as it was for figure 14, but the change in shock position on figure 16 was less than for figure 14. The reason for this can be readily seen in figure 11. It is the change in signal gain for shock motions upstream and downstream of pressure tap f (located 43 cm downstream from the cowl lip) and represents one of the disadvantages of using p_{56} as a control signal. An improvement in the response of the control could be obtained by linearization of this curve, or ideally, one could use a control signal which is a direct measure of shock position.

Shown in figure 17 is a response of the control with reset for the same type of disturbance as figure 16, and with the shock initially located at the same position. The

magnitude of the disturbance was slightly less than it was for figure 16. For this test, the shock was first returned to its commanded position in 0.16 second and speed was slowly reset to its commanded value within 2.0 seconds as seen by the control door closing to counteract the disturbance door opening. Note that the shock remained near its commanded position during the reset action. The data again demonstrate the control's fast outer loop and slow inner loop.

Command change in shock position - move shock downstream. - Figure 18 shows a response of the control without reset for a step change in shock position command - moving the shock downstream. A step change was applied to the $p_{56,com}$ summing junction, resulting in an initial positive value for N_{bias}. Fuel flow was initially increased, followed by a response which is characteristic of the response of an underdamped second-order system to a step input. The shock first reached its new commanded position in 0.15 second, along with the change in engine speed. The shock overshot that position by 0.4 centimeter and it took 1.1 seconds to settle within 10 percent of its final value.

Assuming this loop to be predominantly second order, the oscillatory character of all the parameters shown indicates a damped natural frequency of approximately 4.0 hertz and a damping ratio of about 0.2 for the shock position loop. The lower stability is due to the nonlinearity of the p_{56} signal since all other controller gains were the same as for the prior tests. This will be explained more fully in presenting the next figure.

Command change in shock position - move shock upstream. - Shown in figure 19 is a response of the control without reset for a command change in shock position - moving the shock upstream. For this test, speed and the new commanded shock position are reached in 0.34 second with no overshoots. When this figure is compared with figure 18, the effect of the change in p_{56} signal gain for shock motions upstream and downstream of pressure tap f (fig. 11) is quite evident. Note that the gain term K_1 is the same for both tests. However, the response of figure 19 shows no overshoot on either speed or shock position. This shows the effect of the lower effective loop gain.

Command change in shock position, reduced gain. - Figures 20 and 21 show transients similar to figures 18 and 19 except for a reduced gain in the shock position loop. The initial and final values for shock position and speed are approximately the same, but as expected, the transient times are different.

In figure 20 the shock moved downstream to its new position in 0.28 second without overshoot. In figure 18, at the higher gain setting, it took 1.1 seconds for the shock to settle within 10 percent of its final value. In figure 21, the shock moved upstream to its new position in 0.70 second without overshoot, as opposed to 0.34 second in figure 19.

Again, the higher effective loop gain is apparent for the shock moving in the downstream direction. At the lower controller gain setting, approximately critical system damping is obtained for the downstream-moving shock (fig. 20) but for the upstream-moving shock (fig. 21) the system response is sluggish and overdamped. These responses would have exhibited different characteristics if the initial operating point were at pressure tap b of figure 11, where the slope of the curve remains quite constant.

Increase in fuel flow. - Figure 22 shows a response of the control without reset to a disturbance caused by an increase in fuel flow. Note that the shock position controller gain K_1 has been increased such that $K_1/K_{1,des}$ is now equal to 1.5 for this transient and for figure 23.

The disturbance was introduced as a step increase in voltage at the input to the fuel valve servosystem, as illustrated by the $w_{f,d}$ input of figure 13. The sharp increase in w_f caused speed to increase 0.6 percent from its initial operating point, thereby forcing the shock to move 1.3 centimeters downstream from its initial operating point. The control retarded w_f immediately after detection of a speed error signal and a shock position error. This is indicated by the sharp drop in the fuel valve position trace. Speed and shock position were returned to their commanded values within 0.47 second with one slight speed overshoot.

Decrease in fuel flow. - Figure 23 shows a response of the control without reset for a disturbance caused by a decrease in fuel flow. Fuel flow is decreased by a step voltage applied at the input to the fuel valve servosystem. The decrease in w_f caused speed to drop 0.6 percent from its initial value thereby forcing the shock to move 2.1 centimeters upstream from its initial position. After detection of a speed error and a shock position error, the controller increased w_f, correcting for the disturbance and returning speed and shock position to their commanded values in 0.50 second.

The transients have shown that in each case, the control was stable; however, the response times and paths varied considerably. Variations in the responses are ascribed to a combination of the following causes:

(1) Engine dynamics are different for increasing and decreasing speed.

(2) There is a significant change in the gain of throat exit static pressure p_{56} for shock motions upstream and downstream of the initial position used in these tests.

(3) The auxiliary fuel system with its long feedline introduced significant dynamics, as shown in figure 8.

Sinusoidal Responses - Open Loop

The response of the cross-coupled control system is influenced by the open-loop response of speed and pressure p_{56} to fuel flow and airflow disturbances. Figures 24 to

26 show these open-loop responses. The responses have been normalized to remove the long-fuel-line dynamics and the bypass door dynamics.

Response of speed to a change in fuel flow. - Figure 24 shows the open-loop response of engine speed to fuel flow. This response is predominantly a first-order lag with a corner frequency at about 0.4 hertz as evidenced by the 0.7 amplitude ratio and 45° phase lag at 0.4 hertz. The figure also indicates that in order to obtain a closed-loop response of wide bandwidth, a complicated (higher than first order) controller might be necessary to overdrive the engine. Since the purpose of this program was merely to present a concept, little effort was put into investigating various controller types to achieve wide bandwidth.

Response of throat exit pressure to a change in diffuser exit airflow. - Figure 25 shows the open-loop response of pressure p_{56} to an inlet airflow disturbance. The airflow disturbance was generated by sinusoidally driving the disturbance bypass doors. This figure shows that this response is also predominantly a first-order lag at low frequencies, as evidenced by the 0.7 amplitude ratio and 50° phase lag at 13.5 hertz. The first-order lag is attributed to the inlet volume. At higher frequencies, the curves of figure 25 show the effects of dead time and second-order terms.

Response of throat exit pressure to a change in fuel flow. - The open-loop response of pressure p_{56} to a fuel flow disturbance is shown in figure 26. These data were obtained by sinusoidally disturbing fuel flow, thereby causing speed changes and inlet airflow changes and, hence, changes in pressure p_{56}. A comparison of figure 26 with figures 24 and 25 shows that the transfer function represented by figure 26 is approximately the product of the transfer functions represented by figures 24 and 25. This demonstrates that, for small disturbances, engine speed is proportional to engine airflow.

Sinusoidal Responses - Closed Loop

The closed-loop responses of the control with only the speed loop closed, and with the speed loop and shock position loop closed, are shown in figures 27 to 29 and are discussed in the following paragraphs. Closed-loop frequency response data were not taken for the entire control with reset. The closed-loop frequency response data were taken beginning at 1 hertz. Since it is desirable to know what the response would be below 1 hertz, an analysis has been performed in appendix A to predict this response. Only the results from appendix A are presented in the text.

Response of speed to a change in speed command. - The closed-loop response of speed to speed command with only the speed loop closed is shown in figure 27. The closed-loop speed response, normalized to its 1-hertz value is shown as the solid line on

these figures; the dash-dot line is the open-loop response of speed to a fuel flow disturbance (taken from fig. 24) and is shown for comparison. The short-dashed line is the response of fuel spray nozzle pressure to fuel valve command (taken from fig. 8), and is shown to remind the reader that the auxiliary fuel system with its long lines had dynamics which would affect the closed-loop speed response above 6 hertz. The long-dashed line is the expected response below 1 hertz according to the analysis in appendix A.

From appendix A, the transfer function for determining the shape of this response below 1 hertz is given by

$$\frac{\Delta N}{\Delta N_{com}} = \frac{T_2 s + 1}{\frac{T_6}{K_a} s^2 + \left(T_2 + \frac{1}{K_a}\right) s + 1} \tag{A3}$$

where

$$K_a \triangleq K_2 K_5 K_6$$

Equation (A3) indicates that the low-frequency normalized amplitude ratio would approach a magnitude of 1 and the phase would approach zero degrees; hence, the long-dashed line has been added to represent this.

At 11 hertz, the data show that the closed-loop response of speed to speed command has an amplitude ratio of 0.7 and a phase angle of -190°. The high phase lag (-190°) at an amplitude ratio of 0.7 indicates that the closed-loop speed control is more complicated than the simple approximations used in developing equation (A3). Dead time, for example, in the combustor, and higher-order dynamics above 15 hertz could account for the high phase lag at an amplitude ratio of 0.7. Comparing the closed-loop amplitude ratio to the open-loop amplitude ratio, it is seen that the bandwidth has been extended considerably.

Response of speed to a fuel flow disturbance. - The closed-loop response of speed to a fuel flow disturbance, with only the speed loop closed, is shown in figure 28. The solid line is the closed-loop response and has been normalized to the open-loop dc value. The dash-dot line is the open-loop response of speed to fuel flow, normalized to the open-loop dc value without removing the dynamics caused by the long fuel feedline. The open-loop response is shown for comparison.

The expected closed-loop response below 1 hertz has not been drawn in because it is not known where the curves approach their low-frequency shape. However, according to the analysis in appendix A, the general form of the transfer function for this closed-loop frequency response at low frequencies is given by

$$\frac{\Delta N}{\Delta w_{f,d}} = \frac{\frac{K_6}{K_a} s}{\frac{T_6}{K_a} s^2 + \left(T_2 + \frac{1}{K_a}\right) s + 1} \tag{A4}$$

where

$$K_a \triangleq K_2 K_5 K_6$$

For low frequencies, equation (A4) should have an amplitude ratio curve which approaches a straight line with a positive slope of 1, and the phase curve should approach a 90^o lead.

Response of throat exit pressure to a change in diffuser exit airflow. - Consideration will now be given to the response of the control with both the speed loop and the shock position loop closed. The solid line in figure 29 shows the response of pressure p_{56} to a change in disturbance airflow at the diffuser exit using both control loops. The dash-dot line is the same response obtained without the control and is shown for comparison.

According to the analysis in appendix A, the transfer function for this closed-loop response for low frequencies is given by

$$\frac{\Delta p_{56}}{\Delta w_d} = \frac{\frac{K_8}{K_b} s \left[\frac{T_6}{K_a} s^2 + \left(T_2 + \frac{1}{K_a}\right) s + 1\right]}{\frac{T_6 T_8}{K_a K_b} s^4 + \frac{1}{K_b}\left(T_2 T_8 + \frac{T_6 + T_8}{K_a}\right) s^3 + \frac{1}{K_b}\left(T_2 + T_8 + \frac{1}{K_a} + K_b T_1 T_2\right) s^2 + \frac{1}{K_b}\left[1 + K_b (T_1 + T_2)\right] s + 1} \tag{A5}$$

where

$$K_a \triangleq K_2 K_5 K_6$$

$$K_b \triangleq K_1 K_4 K_7 K_8$$

At low frequencies, the response of $\Delta p_{56}/\Delta w_d$ would show that the amplitude ratio

approaches a straight line with a positive slope of 1, and the phase would approach a 90^{o} lead. This is represented by the dashed line in figure 29.

The closed-loop response shows the desired attenuation for frequencies to about 1.3 hertz, followed by a resonance to about 5 hertz, after which the closed-loop response essentially follows the open-loop response. Use of higher controller gains in this control, to improve the low-frequency response, would amplify the resonance and could cause instability; this could result in inlet unstart. The peaking between 1.3 and 5 hertz is undersirable and suggests that a more complicated control is warranted for a flight application.

CONCLUDING REMARKS

A control system using manipulation of both bypass door flow area and engine speed to stabilize normal shock position in the inlet was designed. It has been shown experimentally that this cross-coupled inlet and engine control is a feasible propulsion system control. This concept could be used as the primary control with a very slow or simplified bypass door system, or it could be used as an inlet backup control mode on failure of the bypass door system. Such a control may offer weight, complexity, and cost advantages as compared to conventional separate inlet and engine controls.

The control system performed stably for downstream disturbances caused by both step-type inputs and swept frequency inputs. Disturbances were applied to diffuser exit airflow, to changes in the commanded value of shock position, and to changes in the value of commanded speed and fuel flow.

No attempt was made to optimize the control system presented herein. The control used produced an engine speed controlled response with cutoff at 10.5 hertz and a normal shock position regulation better than open loop to 1.4 hertz.

Lewis Research Center,
National Aeronautics and Space Administration,
Cleveland, Ohio, October 12, 1970,
720-03.

APPENDIX A

DERIVATION OF THE SHAPE OF THE CLOSED-LOOP FREQUENCY RESPONSE FOR LOW FREQUENCIES

Data were not taken below 1 hertz for the closed-loop responses presented in the text. Since it is desirable to know how the control would behave over the entire frequency range, a simplified analysis is presented here to approximate the shape of the low-frequency closed-loop frequency response data.

Figure 30 is a simplified block diagram of the two-loop control. The engine dynamics, shown as G_6 in the diagram, has the form

$$G_6 = \frac{K_6}{T_6 s + 1} \tag{A1}$$

The inlet dynamics, shown as G_8 in the diagram, has the form

$$G_8 = \frac{K_8}{T_8 s + 1} \tag{A2}$$

These forms are based on figures 24 and 25 which indicate that, from zero to about 10 hertz, both the engine and the inlet exhibit the characteristics of a first-order lag. For small perturbations, engine speed is proportional to engine airflow and this is represented by the constant K_7. The constant K_4 represents a gain term converting the output voltage of the shock position controller to a speed bias signal, and K_5 is the conversion of the output of the speed controller to a fuel flow signal. The light line represents the speed loop and the heavy line represents the shock position loop.

When only the speed loop is considered, the transfer function relating speed to speed command is

$$\frac{\Delta N}{\Delta N_{com}} = \frac{T_2 s + 1}{\frac{T_6}{K_a} s^2 + \left(T_2 + \frac{1}{K_a}\right) s + 1} \tag{A3}$$

where

$$K_a \triangleq K_2 K_5 K_6$$

For this transfer function, the normalized low-frequency amplitude ratio approaches 1 and the phase shift approaches zero degrees. Also, for the speed loop only, the transfer function relating speed to a fuel flow disturbance is

$$\frac{\Delta N}{\Delta w_{f,d}} = \frac{\frac{K_6}{K_a} s}{\frac{T_6}{K_a} s^2 + \left(T_2 + \frac{1}{K_a}\right) s + 1} \tag{A4}$$

where

$$K_a \triangleq K_2 K_5 K_6$$

For low frequencies, $\Delta N/\Delta w_{f,d}$ has an amplitude ratio which approaches a straight line with a positive slope of 1 and the phase approaches a 90^o lead.

When both the speed loop and the shock position loop are considered, the transfer function relating pressure p_{56} to a diffuser exit airflow disturbance is

$$\frac{\Delta p_{56}}{\Delta w_d} = \frac{\frac{K_8}{K_b} s \left[\frac{T_6}{K_a} s^2 + \left(T_2 + \frac{1}{K_a}\right) s + 1\right]}{\frac{T_6 T_8}{K_a K_b} s^4 + \frac{1}{K_b}\left(T_2 T_8 + \frac{T_6 + T_8}{K_a}\right) s^3 + \frac{1}{K_b}\left(T_2 + T_8 + \frac{1}{K_a} + K_b T_1 T_2\right) s^2 + \frac{1}{K_b}\left[1 + K_b(T_1 + T_2)\right] s + 1} \tag{A5}$$

where

$$K_a \triangleq K_2 K_5 K_6$$

$$K_b \triangleq K_1 K_4 K_7 K_8$$

The response of $\Delta p_{56}/\Delta w_d$ for low frequencies would have an amplitude ratio curve which would approach a straight line with a positive slope of 1 and the phase would approach a 90^o lead.

APPENDIX B

SYMBOLS

G	controller transfer function
H	inlet total pressure, N/cm^2
K	controller constant
m	air mass flow, kg/sec
N	engine speed, rpm
p	static pressure, N/cm^2
SP	shock position
s	Laplace transform variable, 1/sec
T	time constant, sec
w	fuel mass flow, kg/hr
x	position, cm
Δ	denotes incremental change

Subscripts:

by	bypass
bias	biasing signal
c	controlled signal
com	commanded signal
d	disturbance
de	diffuser exit
des	design or nominal value
eng	engine
f	fuel flow
max	maximum
new	new value
old	old value
sn	fuel spray nozzle
tot	total
v	fuel valve
0	freestream conditions
1,...,8	controller constants
56	at the throat exit 56.13 cm downstream of the cowl lip

REFERENCES

1. Crosby, Michael J.; Neiner, George H.; and Cole, Gary L.: Restart and High Response Terminal Shock Control For An Axisymmetric Mixed-Compression Inlet With 60-Percent Internal Contraction. NASA TM X-1792, 1969.

2. Chun, K. S.; and Burr, R. H.: A Control System Concept and Substantiation Test For An Axisymmetric Mixed-Compression Supersonic Inlet. Paper 68-581, AIAA, June 1968.

3. Martin, Arnold W.: Propulsion System Flow Stability Program (Dynamic). Part 1: Summary, Phase 2. Rep. NA-69-870, pt. 1, North American Rockwell Corp. (AFAPL-TR-69-113, pt. 1, DDC No. AD-866497), Feb. 1970.

4. Cole, Gary, L.; Neiner, George H.; Wallhagen, Robert E.: Coupled Supersonic Inlet-Engine Control Using Overboard Bypass Doors and Engine Speed to Control Normal Shock Position. NASA TN D-6019, 1970.

5. Cubbison, Robert W.; Meleason, Edward T.; and Johnson, David F.: Effect of Porous Bleed in a High-Performance Axisymmetric, Mixed-Compression Inlet at Mach 2.50. NASA TM X-1692, 1968.

6. Cubbison, Robert W.; Meleason, Edward T.; and Johnson, David F.: Performance Characteristics From Mach 2.58 to 1.98 of an Axisymmetric, Mixed-Compression Inlet System With 60-Percent Internal Contraction. NASA TM X-1739, 1969.

7. Sanders, Bobby W.; and Cubbison, Robert W.: Effect of Bleed-System Back Pressure and Porous Area on the Performance of an Axisymmetric Mixed-Compression Inlet at Mach 2.50. NASA TM X-1710, 1968.

8. Coltrin, Robert E.; and Choby, David A.: Steady-State Interactions From Mach 1.98 to 2.58 Between a Turbojet Engine and an Axisymmetric Inlet With 60-Percent Internal Area Contraction Systems. NASA TM X-1780, 1969.

9. Wasserbauer, Joseph F.: Dynamic Response of a Mach 2.5 Axisymmetric Inlet With Engine or Cold Pipe and Utilizing 60 Percent Supersonic Internal Area Contraction. NASA TN D-5338, 1969.

10. Zeller, John R.: Design and Analysis of a Modular Servoamplifier For Fast-Response Electrohydraulic Control Systems. NASA TN D-4898, 1968.

11. Batterton, Peter G.; and Zeller, John R.: Dynamic Performance Analysis of a Fuel-Control Valve For Use in Airbreathing Engine Research. NASA TN D-5331, 1969.

12. Cole, Gary L.; Neiner, George H.; and Crosby, Michael J.: Design and Performance of a Digital Electronic Normal Shock Position Sensor For Mixed-Compression Inlets. NASA TN D-5606, 1969.

13. Drain, Daniel I.; Bruton, William M.; and Paulovich, Francis J.: Airbreathing Propulsion System Testing Using Sweep Frequency Techniques. NASA TN D-5485, 1969.

TABLE I. - SUMMARY OF TRANSIENT RESPONSES

[Shock position, distance from cowl lip, 42.7 cm.]

Figure	Type of disturbance	Initial conditions			Shock position controller gain, $K_1/K_{1,des}$	Speed reset loop
		Inlet total-pressure recovery	Percent corrected engine speed	Compressor pressure ratio		
14	Decrease bypass corrected airflow	0.86	86.3	4.13	1.0	Absent
15		0.87	86.7	4.18	1.0	Present
16	Increase bypass corrected airflow	0.86	87.3	4.13	1.0	Absent
17		0.87	86.7	4.18	1.0	Present
18	Command change in shock position - move shock downstream	0.87	86.4	4.13	1.0	Absent
19	Command change in shock position - move shock upstream	0.87	86.4	4.13	1.0	Absent
20	Command change in shock position - move shock downstream	0.87	86.4	4.13	0.5	Absent
21	Command change in shock position - move shock upstream	0.87	86.4	4.13	0.5	Absent
22	Disturbance in fuel flow - increase fuel flow	0.87	86.4	4.13	1.5	Absent
23	Disturbance in fuel flow - decrease fuel flow	0.87	86.4	4.13	1.5	Absent

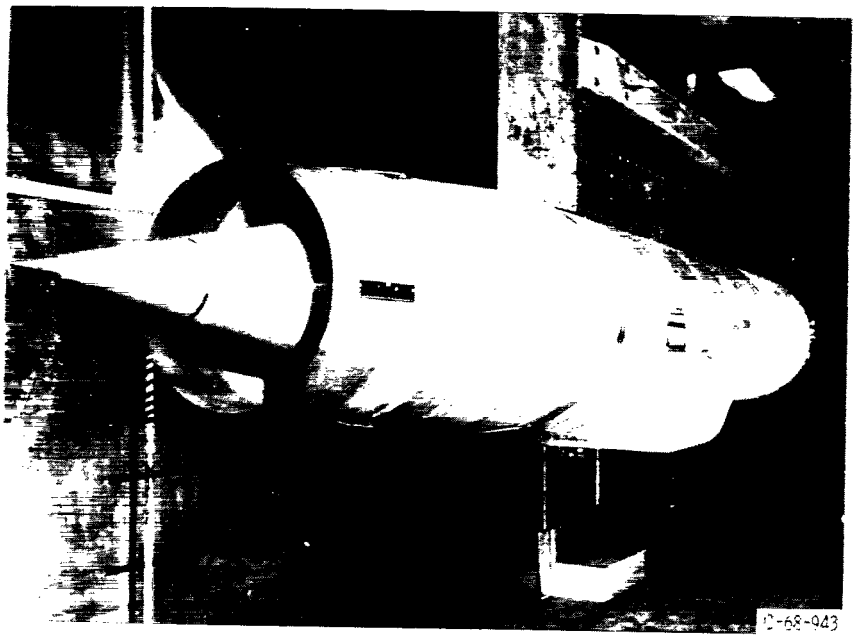

Figure 1. - Engine and inlet, with nacelle, installed in wind tunnel.

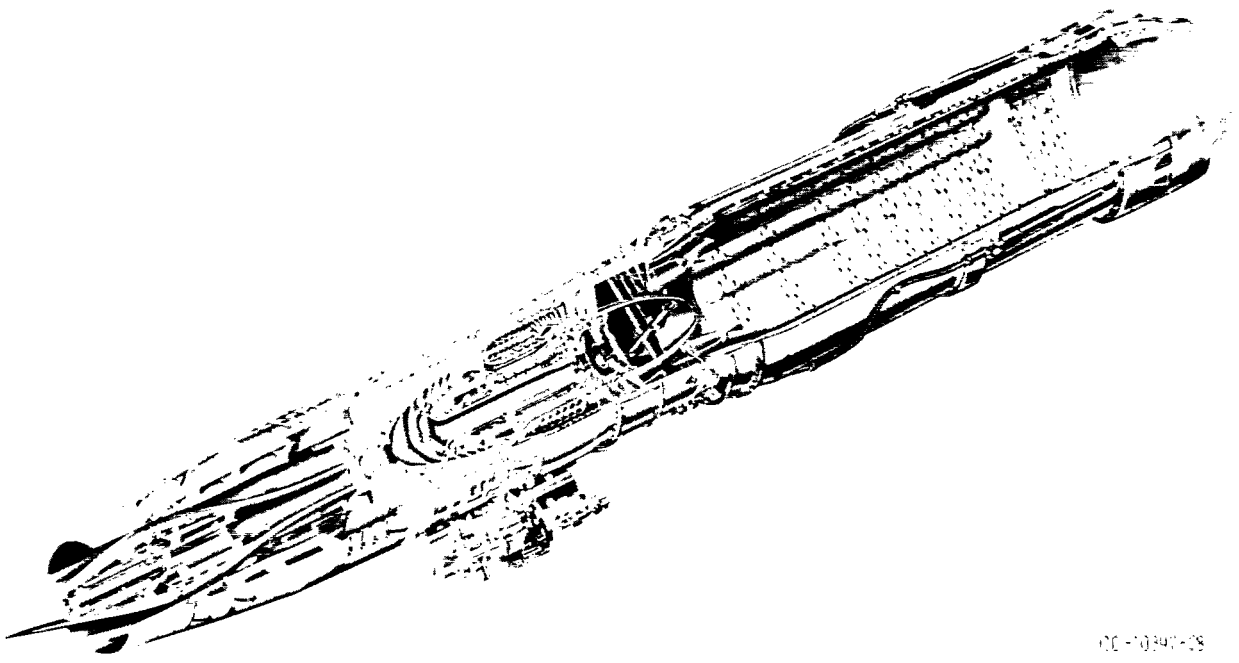

Figure 2. - Cutaway view of engine and inlet.

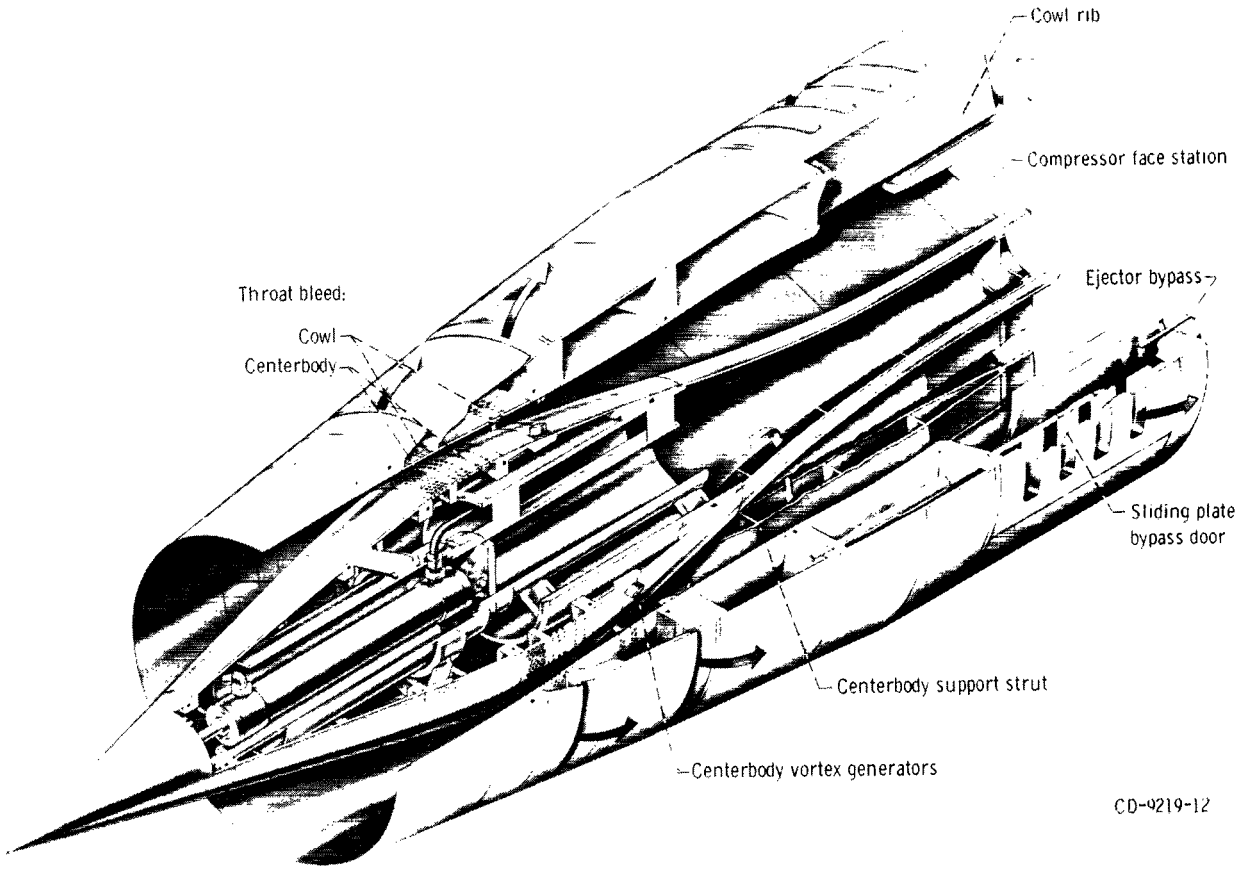

Figure 3. - Cutaway view of inlet.

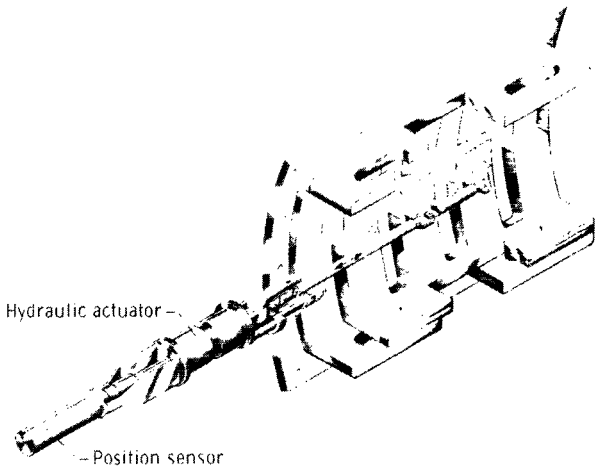

Figure 4. - Sliding-plate overboard bypass door.

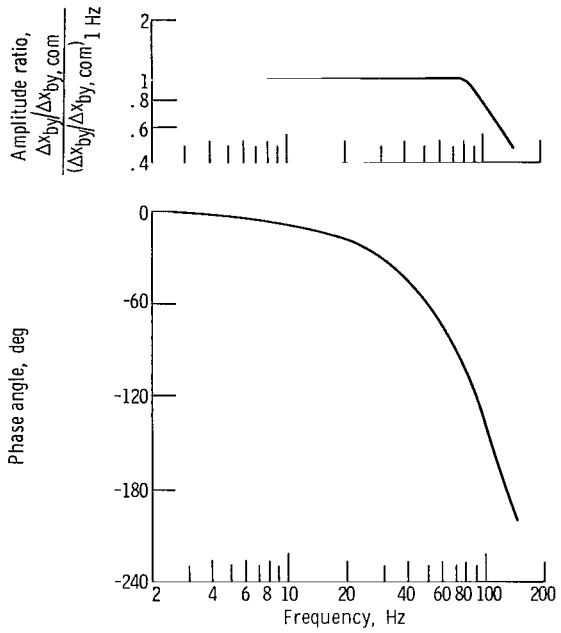

Figure 5. - Response of bypass door displacement to a command in displacement. Zero-to-peak amplitude of command equals 7 percent of full stroke.

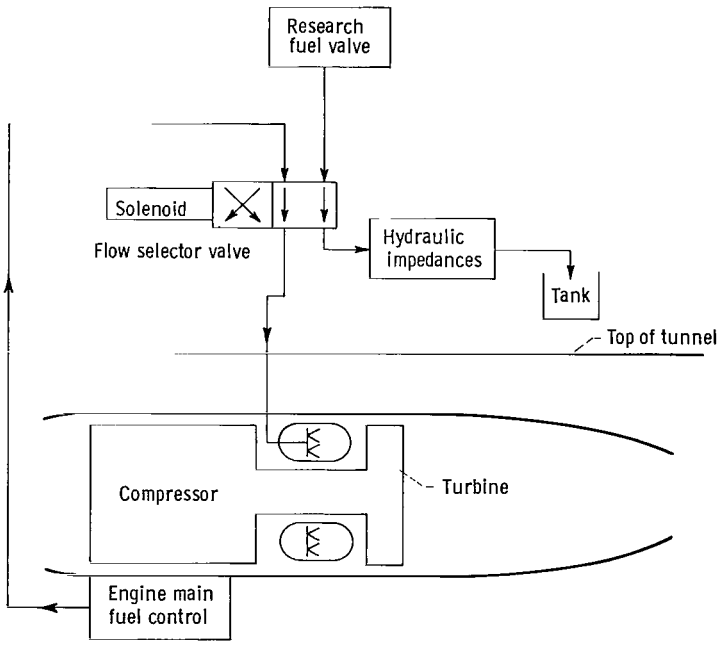

Figure 6. - Schematic of auxiliary fuel system.

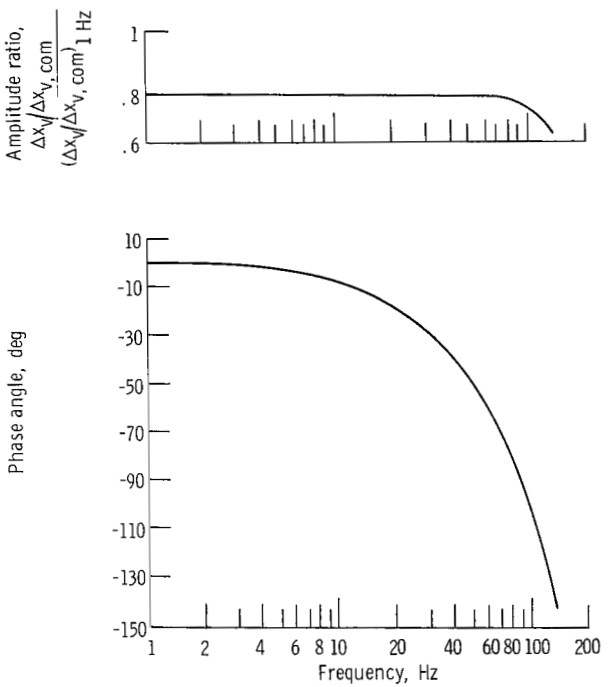

Figure 7. - Frequency response of research-fuel-valve shaft position to command voltage. Valve 15 percent open at operating point; zero-to-peak amplitude of command equals 1.5 percent of full stroke.

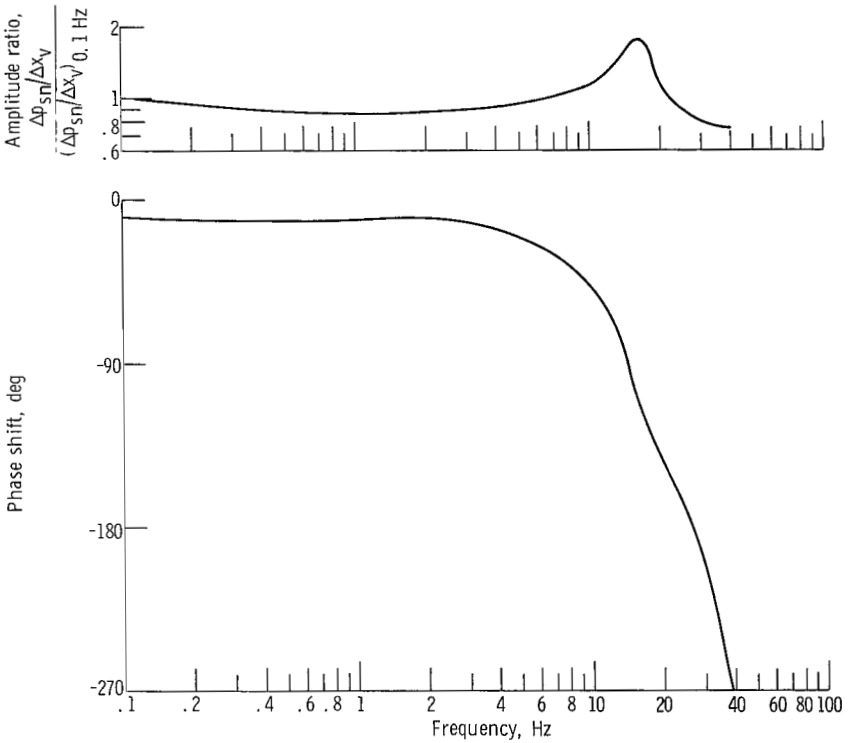

Figure 8. - Frequency response of fuel spray nozzle pressure to fuel valve command. Zero-to-peak amplitude of command equals 1.5 percent.

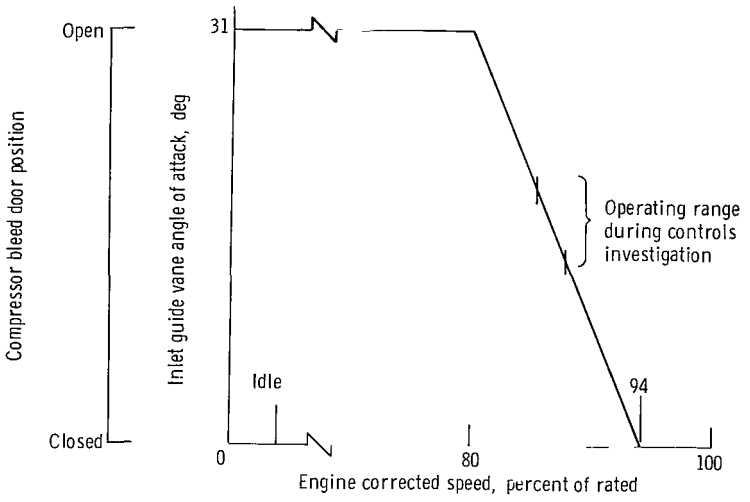

Figure 9. - Compressor variable geometry, normal schedule.

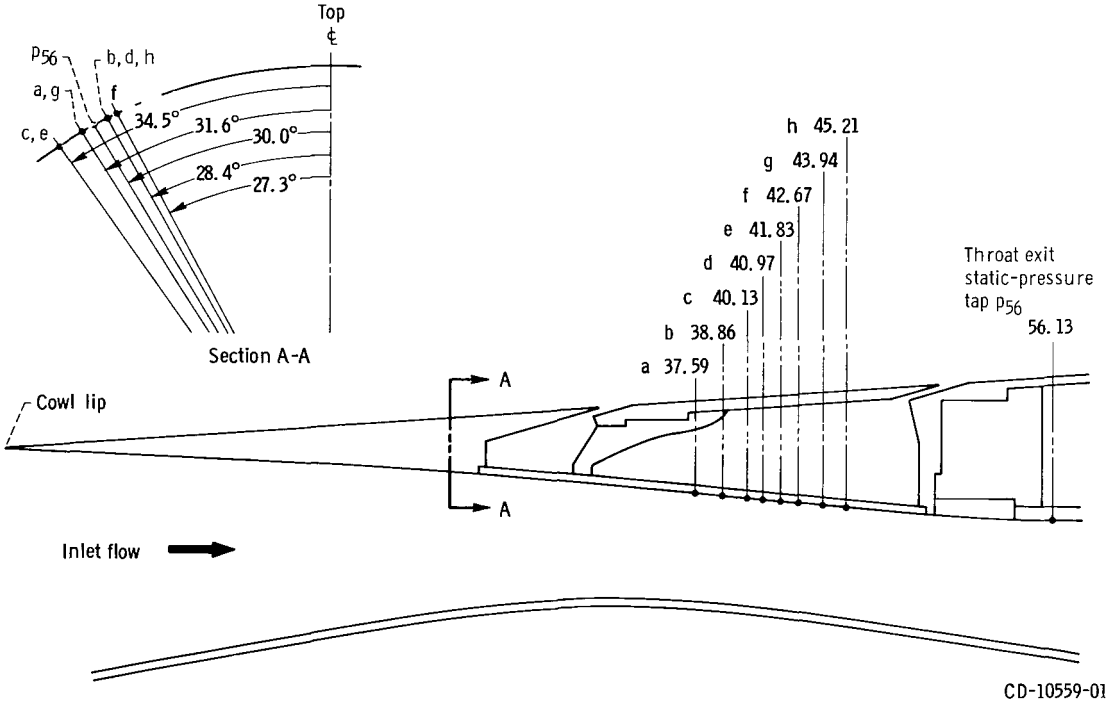

Figure 10. - Inlet throat dynamic instrumentation locations. (Dimensions in centimeters from cowl lip.)

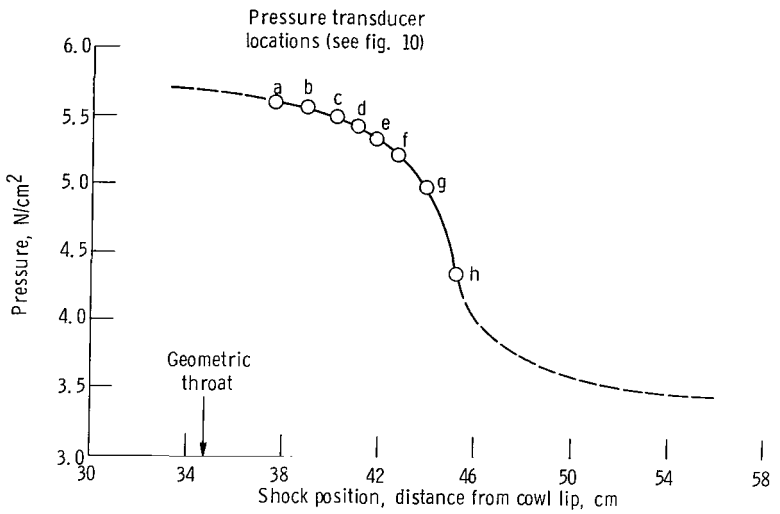

Figure 11. - Throat exit static pressure p_{56}, as a function of shock position. (Dashed portions of curve are extrapolated data.)

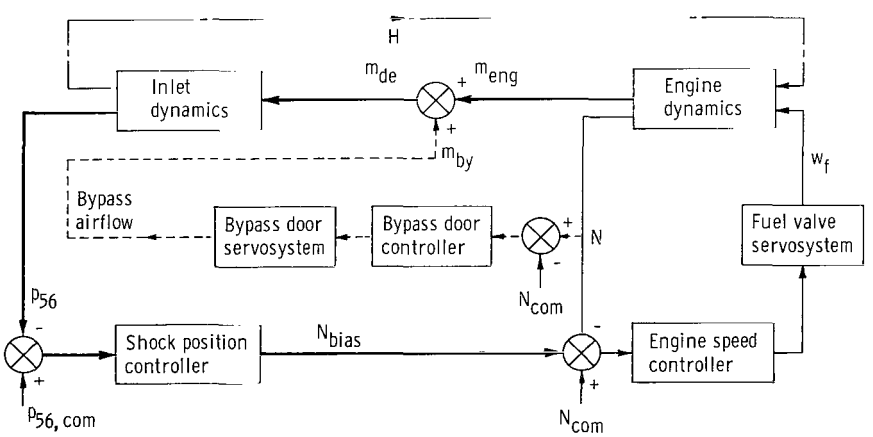

Figure 12. - Simplified block diagram of cross-coupled control.

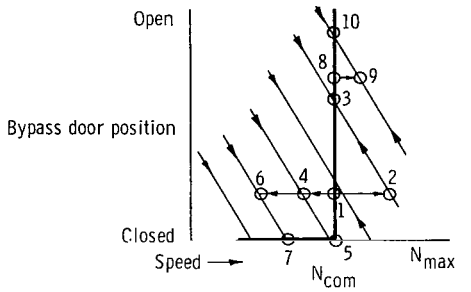

(a) Control action schematic.

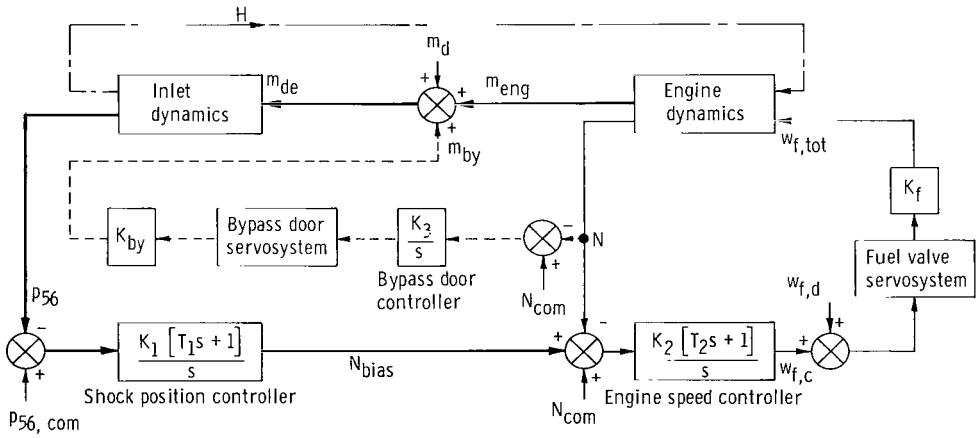

(b) Control block diagram.

Figure 13. - Control block diagram with control action schematic.

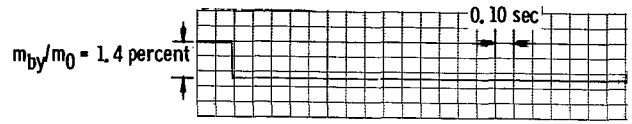

(a) Disturbance bypass door position.

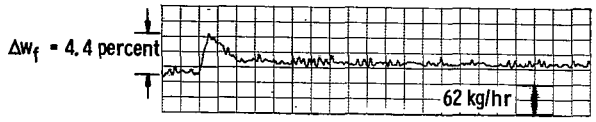

(b) Fuel valve position.

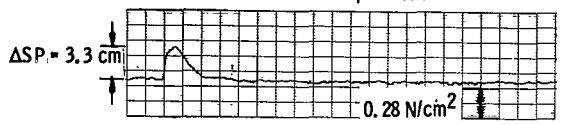

(c) Pressure, p_{56}.

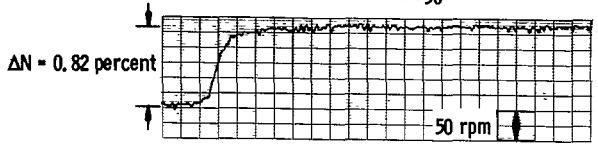

(d) Speed.

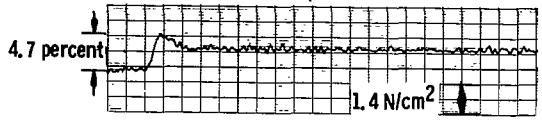

(e) Compressor discharge pressure.

Figure 14. - Response of the control without reset to a decrease in bypass corrected airflow. Shock position controller gain, K_1/K_{des} = 1.0.

(a) Disturbance bypass door position.

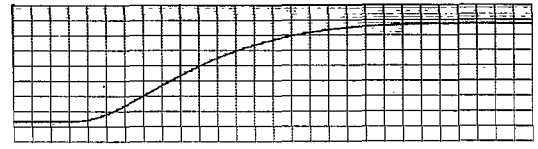

(b) Control bypass door position.

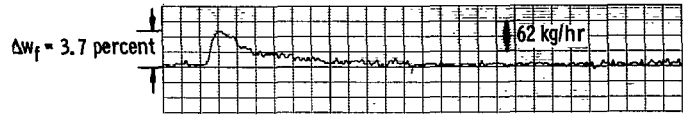

(c) Fuel valve position.

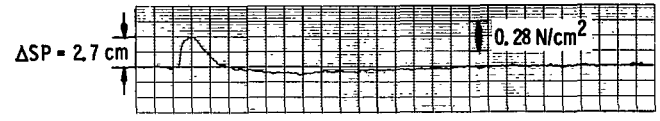

(d) Pressure p_{56}.

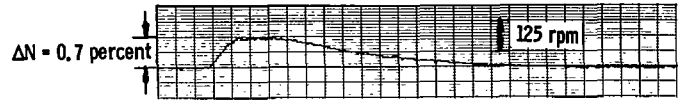

(e) Speed.

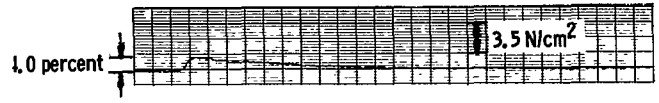

(f) Compressor discharge pressure.

Figure 15. - Response of the control with reset to a decrease in bypass corrected airflow. Shock position controller gain, K_1/K_{des} = 1.0.

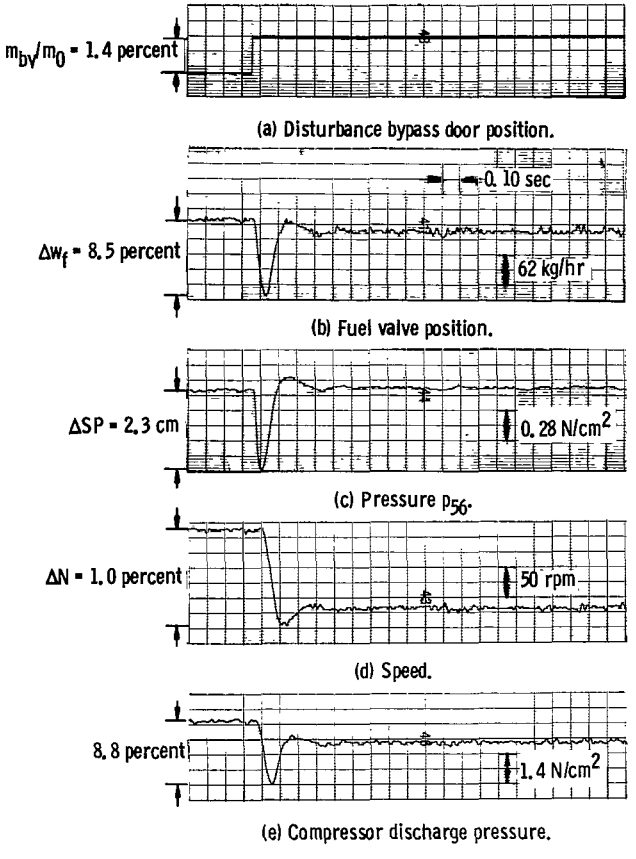

(a) Disturbance bypass door position.

(b) Fuel valve position.

(c) Pressure p_{56}.

(d) Speed.

(e) Compressor discharge pressure.

Figure 16. - Response of the control without reset to an increase in bypass corrected airflow. Shock position controller gain, K_1/K_{des} = 1.0.

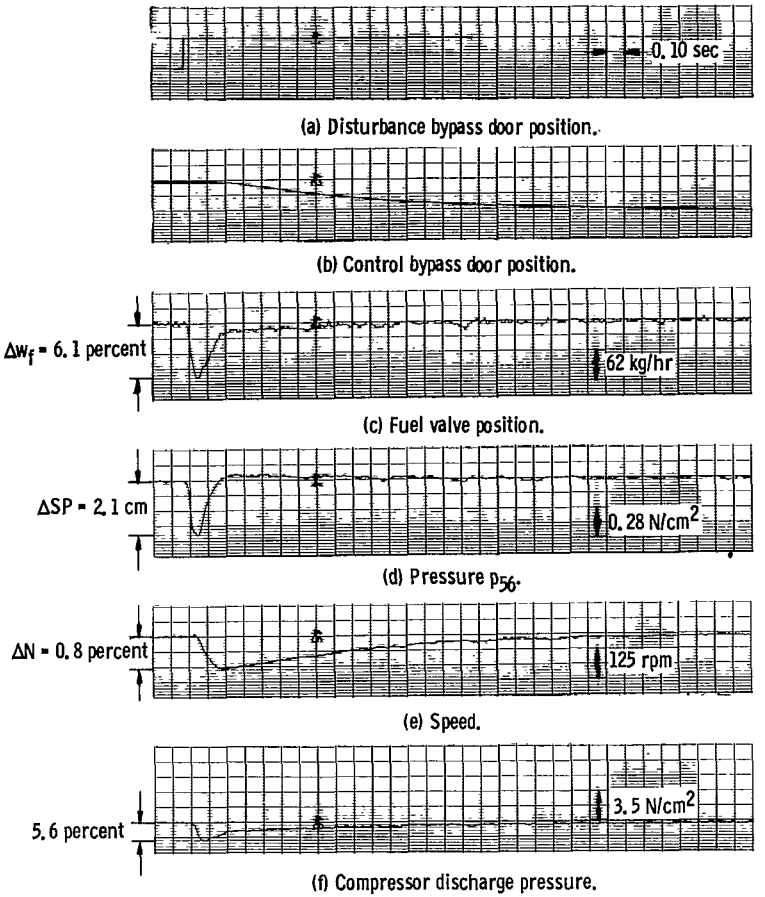

(a) Disturbance bypass door position.

(b) Control bypass door position.

(c) Fuel valve position.

(d) Pressure p_{56}.

(e) Speed.

(f) Compressor discharge pressure.

Figure 17. - Response of the control with reset to an increase in bypass corrected airflow. Shock position controller gain, K_1/K_{des} = 1.0.

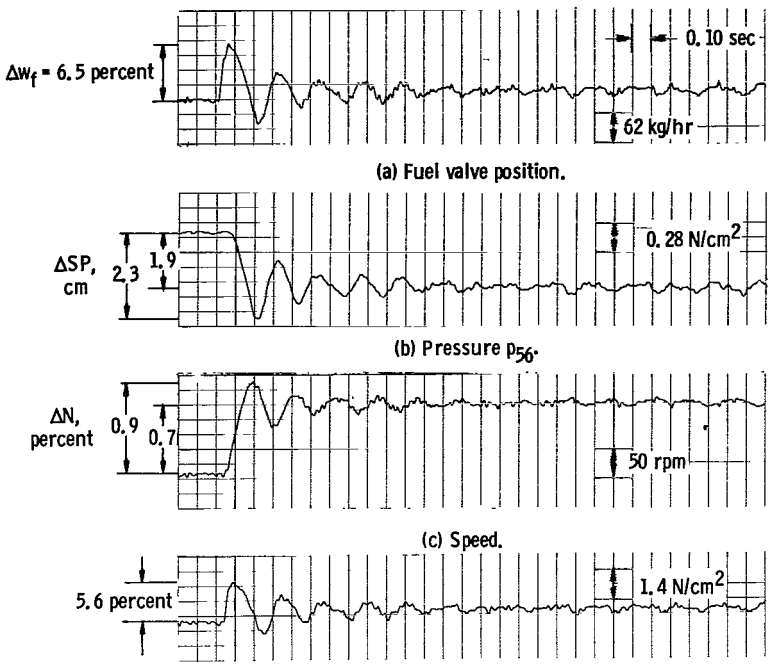

Figure 18. - Response of the control without reset to a command change in shock position, moving the shock downstream. Shock position controller gain, $K_1/K_{1,des}$ = 1.0.

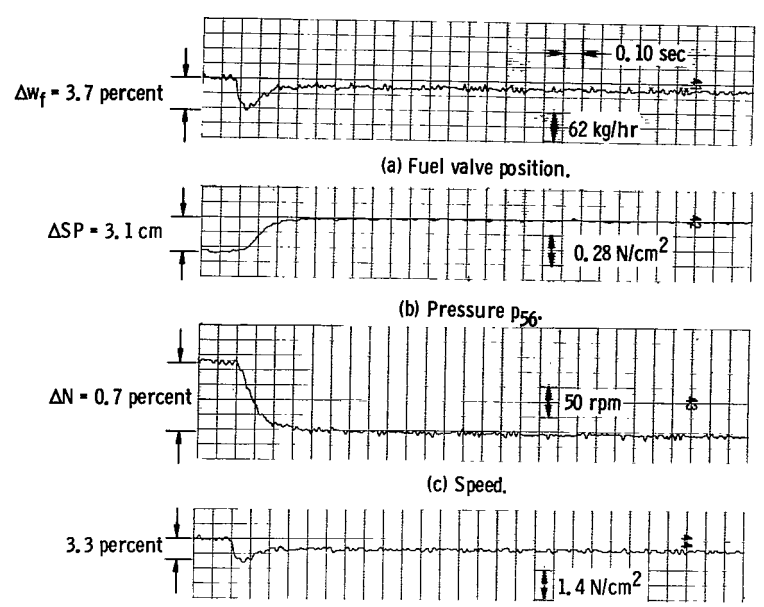

Figure 19. - Response of the control without reset to a command change in shock position, moving the shock upstream. Shock position controller gain, $K_1/K_{1,des}$ = 1.0.

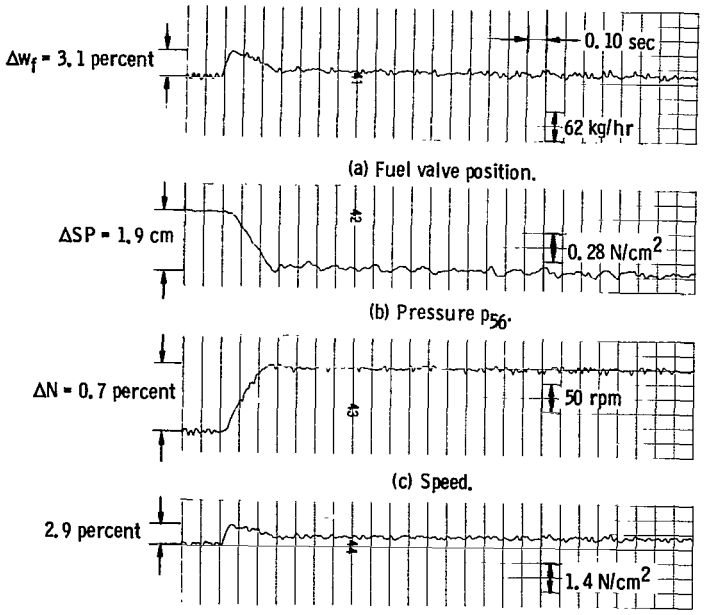

Figure 20. - Response of the control without reset to a command change in shock position, moving the shock downstream. Shock position controller gain, $K_1/K_{1,\,des}$ = 0.5.

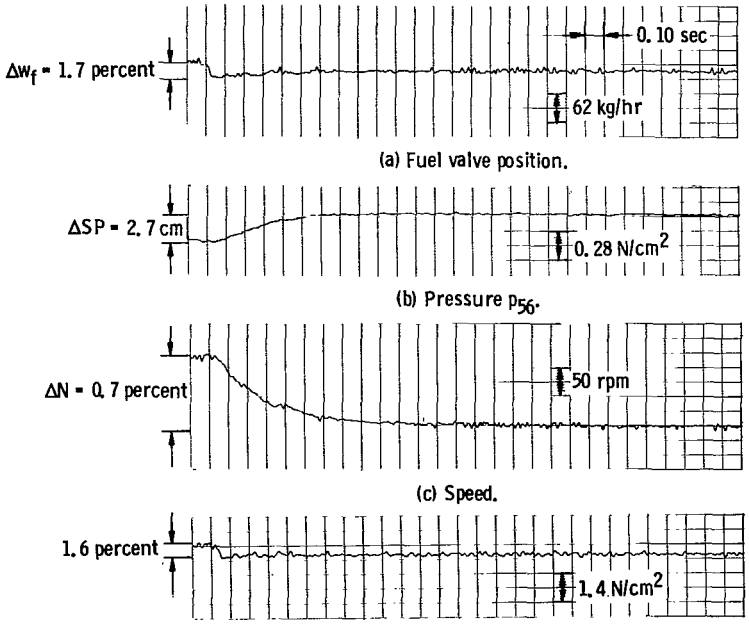

Figure 21. - Response of the control without reset to a command change in shock position, moving the shock upstream. Shock position controller gain, $K_1/K_{1,\,des}$ = 0.5.

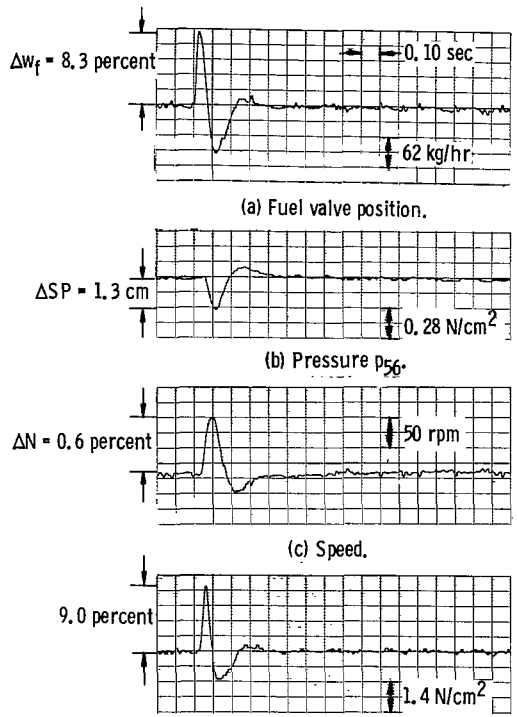

Figure 22. - Response of the control without reset to a disturbance in fuel flow, sharp increase in fuel flow. Shock position controller gain, $K_1/K_{1,des}$ = 1.5.

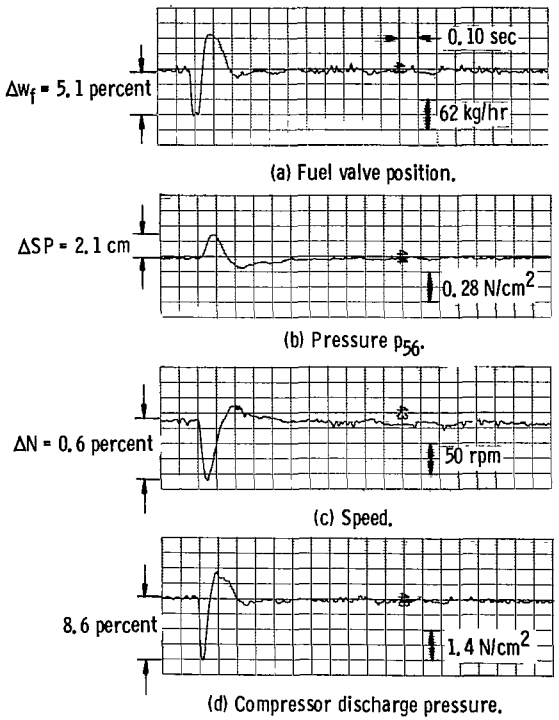

Figure 23. - Response of the control without reset to a disturbance in fuel flow, sharp decrease in fuel flow. Shock position controller gain, $K_1/K_{1,des}$ = 1.5.

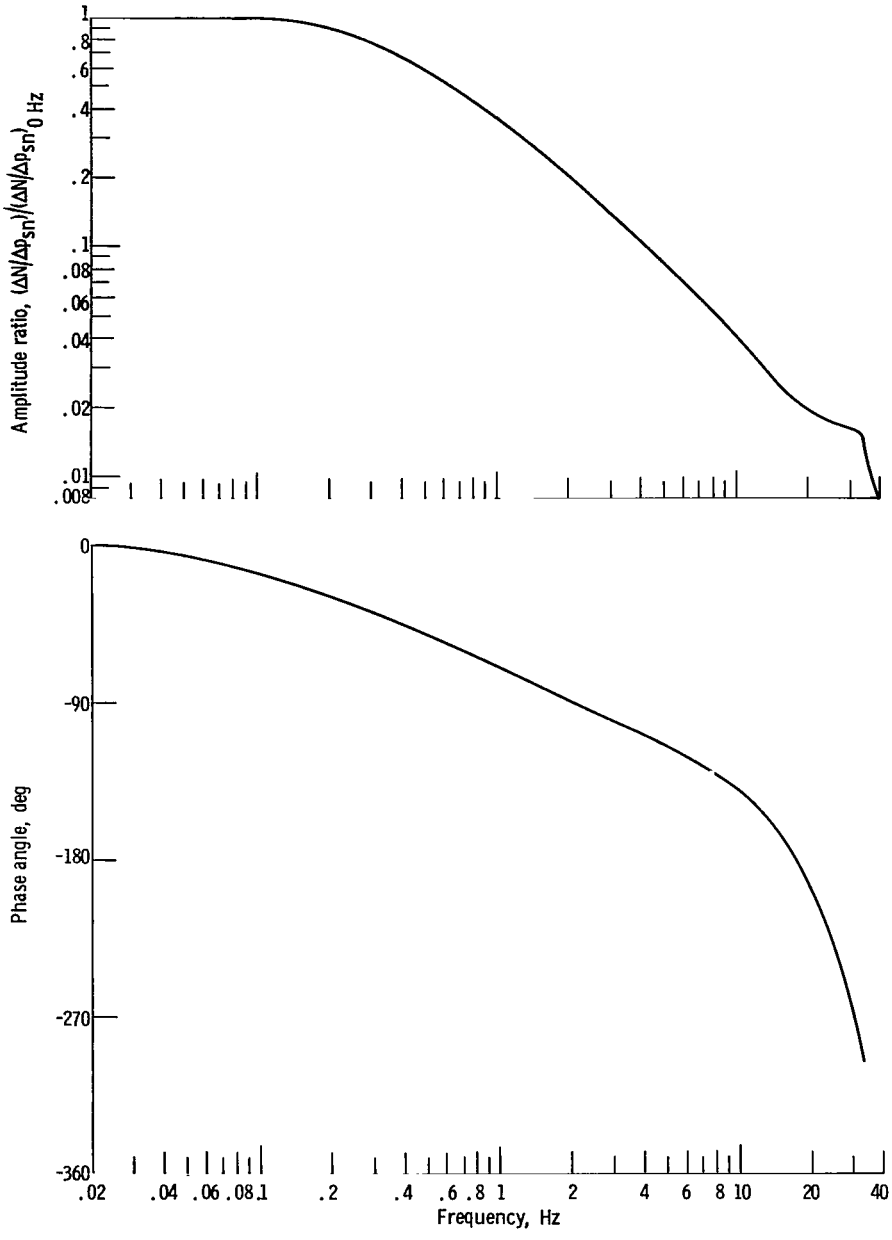

Figure 24. - Response of engine speed to fuel flow - open loop.

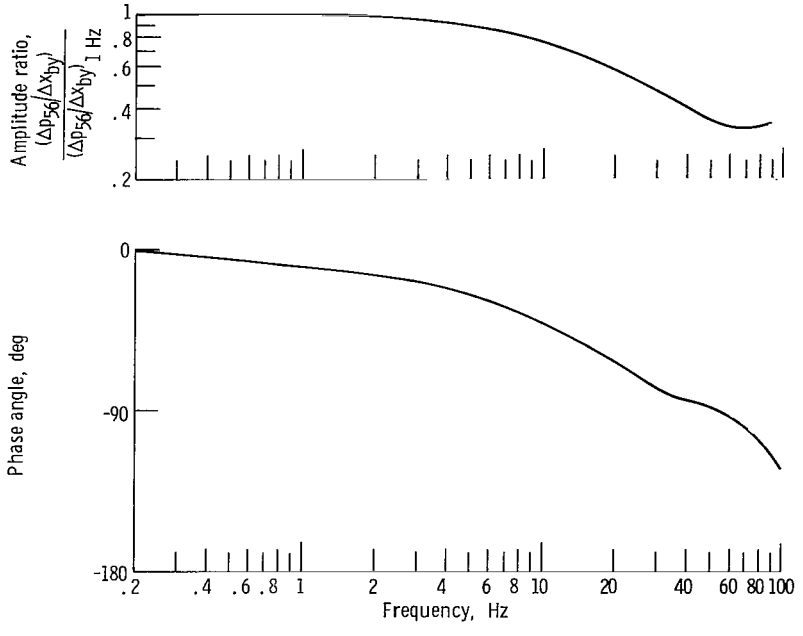

Figure 25. - Response of throat exit static pressure to bypass door position - open loop.

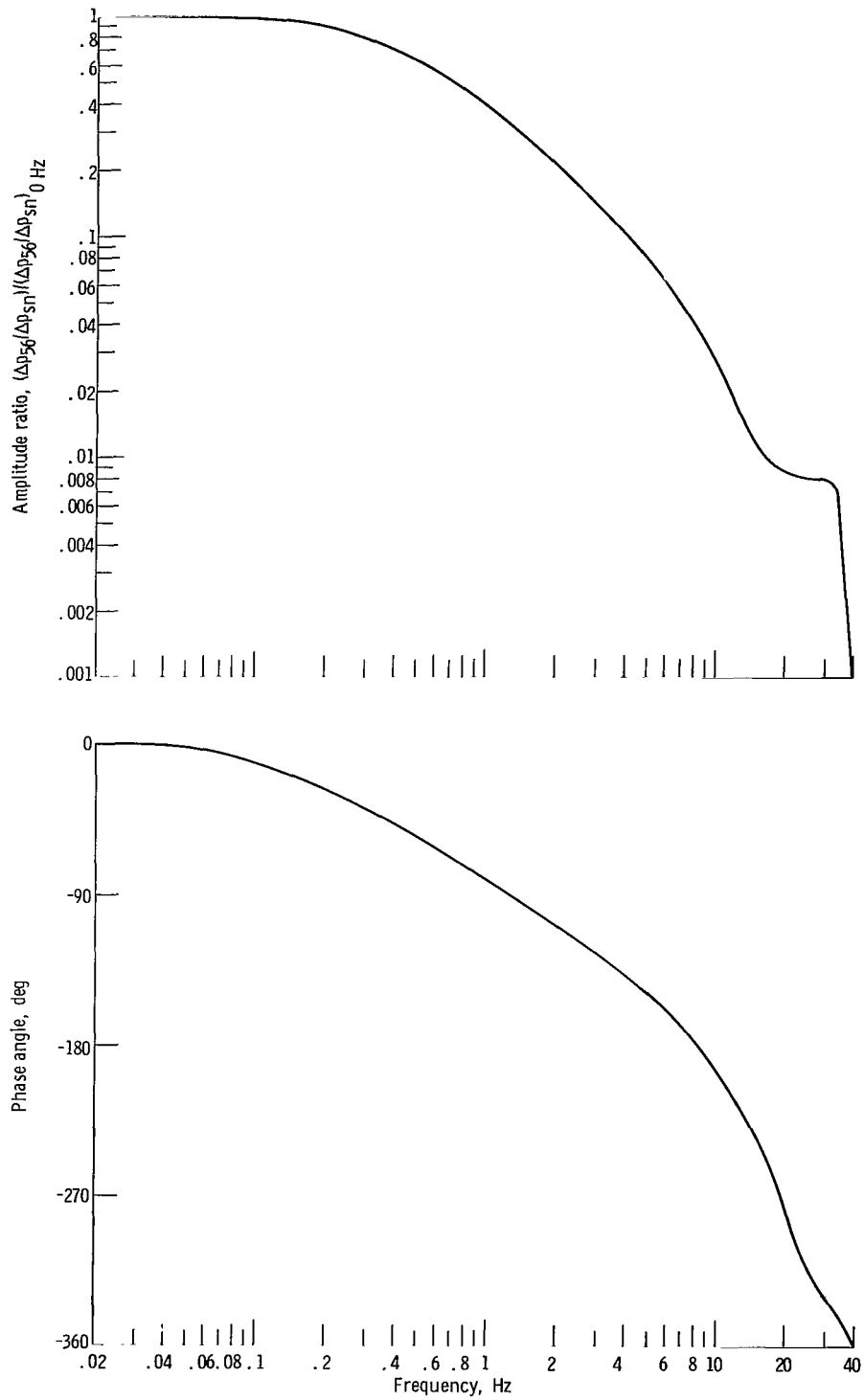

Figure 26. - Response of throat exit static pressure to fuel spray nozzle pressure - open loop.

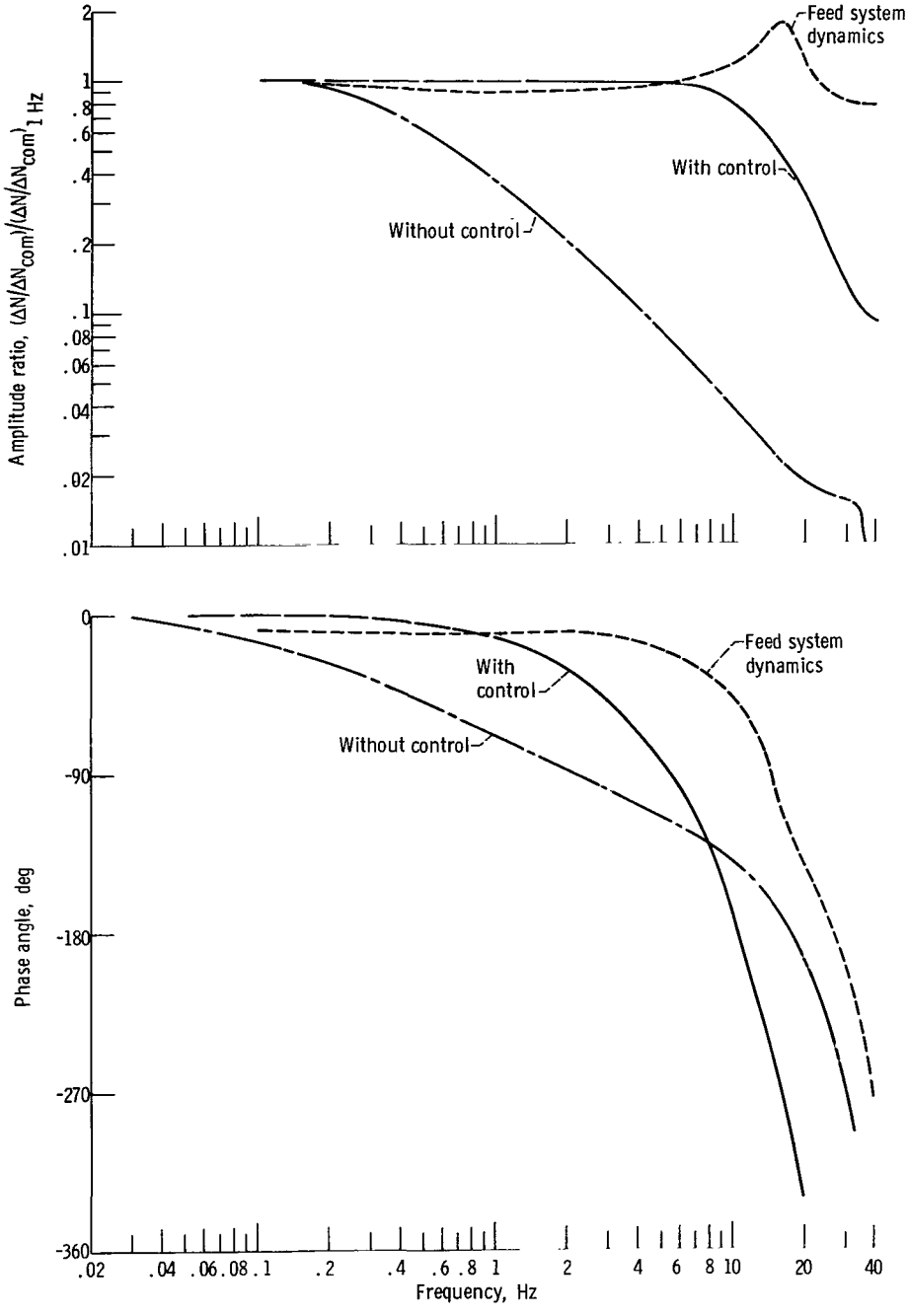

Figure 27. - Response of speed to a change in speed command - with only the speed loop closed.

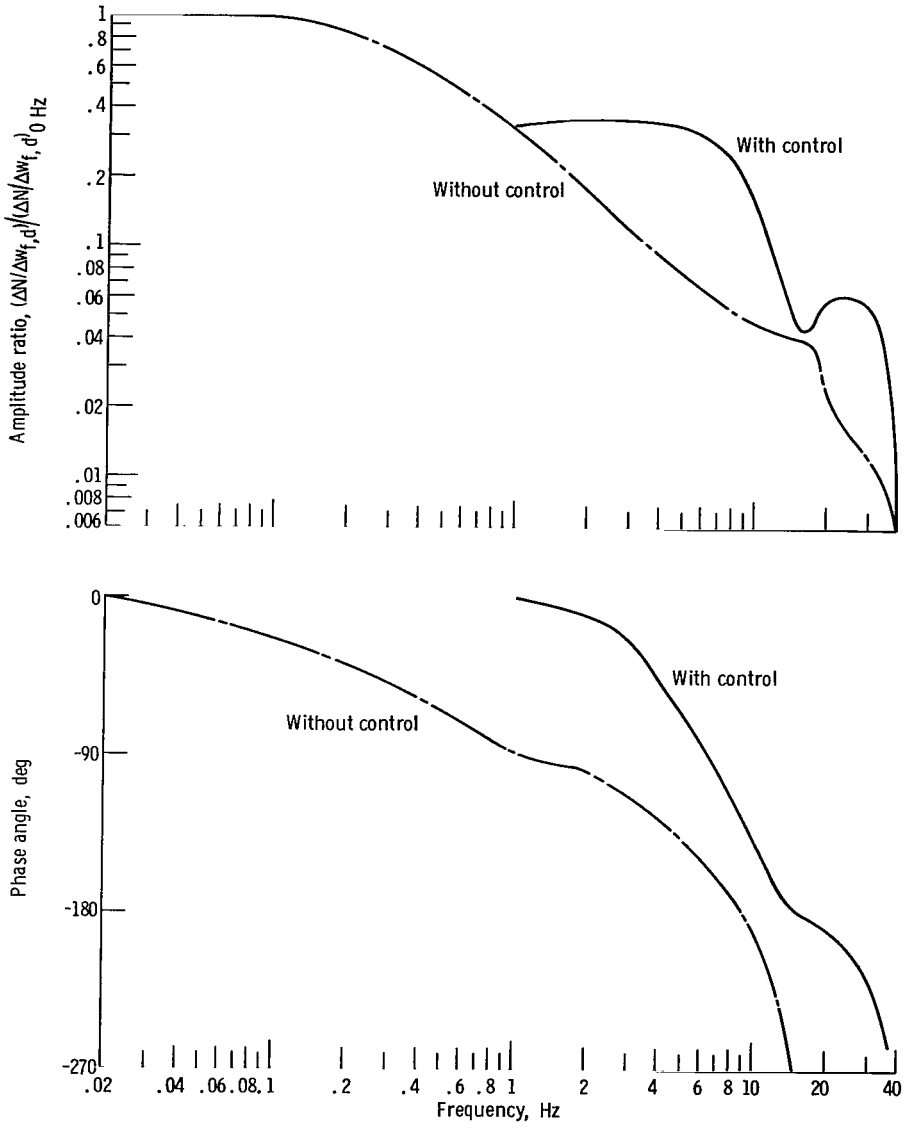

Figure 28. - Response of speed to a fuel flow disturbance - with only the speed loop closed.

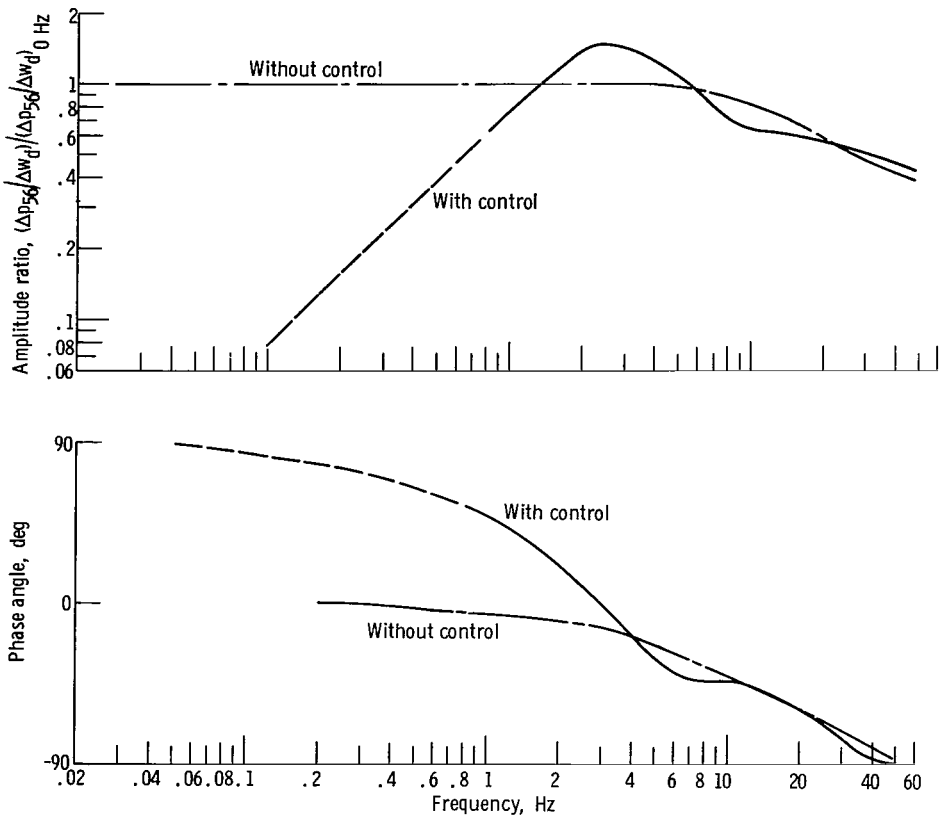

Figure 29. - Response of throat exit static pressure to a bypass door disturbance - with both speed loop and shock position loop closed.

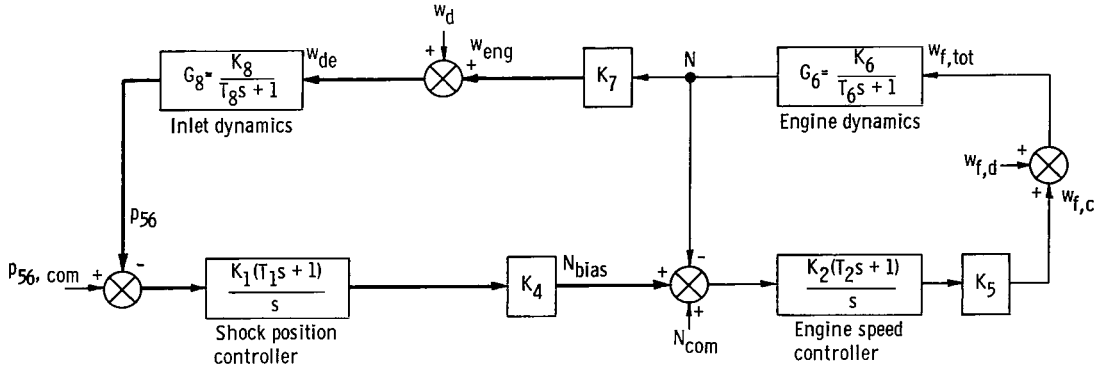

Figure 30. - Simplified block diagram of two-loop control.

NASA-Langley, 1971 —— 5 E-5492

"The aeronautical and space activities of the United States shall be conducted so as to contribute . . . to the expansion of human knowledge of phenomena in the atmosphere and space. The Administration shall provide for the widest practicable and appropriate dissemination of information concerning its activities and the results thereof."

—NATIONAL AERONAUTICS AND SPACE ACT OF 1958

NASA SCIENTIFIC AND TECHNICAL PUBLICATIONS

TECHNICAL REPORTS: Scientific and technical information considered important, complete, and a lasting contribution to existing knowledge.

TECHNICAL NOTES: Information less broad in scope but nevertheless of importance as a contribution to existing knowledge.

TECHNICAL MEMORANDUMS: Information receiving limited distribution because of preliminary data, security classification, or other reasons.

CONTRACTOR REPORTS: Scientific and technical information generated under a NASA contract or grant and considered an important contribution to existing knowledge.

TECHNICAL TRANSLATIONS: Information published in a foreign language considered to merit NASA distribution in English.

SPECIAL PUBLICATIONS: Information derived from or of value to NASA activities. Publications include conference proceedings, monographs, data compilations, handbooks, sourcebooks, and special bibliographies.

TECHNOLOGY UTILIZATION PUBLICATIONS: Information on technology used by NASA that may be of particular interest in commercial and other non-aerospace applications. Publications include Tech Briefs, Technology Utilization Reports and Technology Surveys.

Details on the availability of these publications may be obtained from:

SCIENTIFIC AND TECHNICAL INFORMATION OFFICE

NATIONAL AERONAUTICS AND SPACE ADMINISTRATION

Washington, D.C. 20546